Hindawi
Mathematical Problems in Engineering
Volume 2019, Article ID 7527148, 19 pages
https://doi.org/10.1155/2019/7527148

Research Article

Free Vibration of Functionally Graded Sandwich Shallow Shells on Winkler and Pasternak Foundations with General Boundary Restraints

Xiancheng Wang[1,2] **Wei Li**[1] **Jianjun Yao**[3] **Zhenshuai Wan**[3] **Yu Fu**[3] **and Tang Sheng**[3]

[1]*State Key Laboratory of Fluid Power Transmission and Control, Zhejiang University, Hangzhou 310027, China*
[2]*Ningbo Institute of Technology, Zhejiang University, Ningbo 315100, China*
[3]*College of Mechanical and Electrical Engineering, Harbin Engineering University, Harbin 150001, China*

Correspondence should be addressed to Yu Fu; fuyu@hrbeu.edu.cn

Received 9 January 2019; Accepted 20 February 2019; Published 13 March 2019

Academic Editor: Francesco Tornabene

In this investigation, an exact method based on the first-order shear deformation shallow shell theory (FSDSST) is performed for the free vibration of functionally graded sandwich shallow shells (FGSSS) on Winkler and Pasternak foundations with general boundary restraints. Vibration characteristics of the FGSSS have been obtained by the energy function represented in the orthogonal coordinates, in which the displacement and rotation components consisted of standard double Fourier cosine series and several closed-form supplementary functions are introduced to eliminate the potential jumps and boundary discontinuities. Then, the expansion coefficients are determined by using Rayleigh-Ritz method. The proposed method shows good accuracy and reliability by comprehensive investigation concerning free vibration of the FGSSS. Numerous new vibration results for FGSSS on Winkler and Pasternak foundations with various curvature types, geometrical parameters, and boundary restraints are provided, which may serve as benchmark solutions for future research. In addition, the effects of the inertia, shear deformation, and foundation coefficients on free vibration characteristic of FGSSS are illustrated.

1. Introduction

The functionally graded (FG) materials are widely used in aerospace, automobile, and civil engineering due to continuous variation of material properties along the thickness direction [1–7]. As is known to us, the FG shallow shells-structures, i.e., FG plate, FG circular cylindrical shallow shell, FG spherical shallow shell, and FG hyperbolic paraboloidal shallow shell, have attracted considerable attention for its high strength and stiffness [8–12]. It is noticed that the FG shallow shells are unavoidably suffered from dynamic loads, which can lead to fatigue wear and structural damage [13–15]. Therefore, it is essential to study the free vibration characteristics of FG shallow shell structures.

Recently, extensive research efforts focused on vibration of FG shallow shells have been made by various shell theories, such as classical shallow shell theory (CSST) [16], first-order shear deformation theory (FSDT) [17], and higher-order shear deformation theory (HSDT) [18]. Furthermore, numerous calculation methods, i.e., Ritz method, finite element method (FEM), generalized differential quadrature method, and wave propagation approach, have also been developed [19–27].

Most of the above researches are limited to the classical boundary restraints (clamped, free, simply supported, and shear-diaphragm supported), which requires constant modification of the solution procedure according to the variation of the boundary restraints [28–30]. However, in practical engineering applications, the boundary restraints are not always in certain classical case. There are many possible boundaries such as nonuniform boundaries, elastic edge boundaries, and point-supported boundaries [31–34].

Consequently, an efficient and accurate method for vibration analysis of FG shallow shells with general boundary restraints including classical and elastic edge boundaries is needed. On the other hand, among the FG shallow shells, the existing results of FG sandwich shallow shells (FGSSS) are too scarce for the comparative studies and engineering applications [35–37]. Talebitooti et al. [38] studied the sound transmission across FG laminated sandwich cylindrical shells by using three-dimensional elasticity theory. Hao et al. [39] investigated the nonlinear forced vibrations and natural frequency of FG doubly curved shallow shells with a rectangular base based on the third-order shear deformation theory. Sofiyev [40] presented a modified form of FSDT to solve the bucking problem of FG sandwich truncated conical shells. Trinh and Kim [41] employed the fourth-order Runge-Kutta method to obtain analytical closed-form solutions for thin FGSSS with double curvature testing on elastic bases.

Therefore, this paper presents an exact method for the free vibration of FGSSS on Winkler and Pasternak foundations based on first-order shear deformation shallow shell theory (FSDSST). Regardless of boundaries, the standard double Fourier cosine series and several closed-form supplementary functions are introduced to describe the displacement and rotation components of FGSSS so as to eliminate the possible jumps and boundary discontinuities. The current results are checked by comparing with those results published in other literature. Numerous new vibration results for FGSSS with different curvature types, geometrical parameters, and boundary restraints resting on Winkler and Pasternak foundations are presented. The results show that vibration frequencies of FGSSS are strongly influenced by the boundaries. Furthermore, the effect of inertia, shear deformation, and foundation coefficients on free vibration characteristic is comprehensively investigated by comparing FSDSST with CSST.

2. Materials and Methods

2.1. Model Description and Material Properties. The basic configuration of FGSSS in rectangular planform is depicted in Figure 1. Herein, the length, width, and total thickness are represented by a, b, and h, respectively. The FGSSS considered here are characterized by the middle surface, which can be obtained by [45]

$$z = -\left(\frac{x^2}{2R_x} + \frac{y^2}{2R_y} + \frac{xy}{R_{xy}}\right) \tag{1}$$

where R_x and R_y denote the radii of curvature in the directions of x and y, respectively. R_{xy} is the corresponding radius of twist. In this work, we set R_x, R_y, and R_{xy} as constants. The x and y coordinates are parallel to boundaries so that R_{xy} is infinity. Herein, three types of independent springs including translational, rotational, and torsional springs are used to realize the given boundaries of FGSSS by setting the stiffness of the springs (x=0, a, y=0, b) as various values, which are K_φ^x, K_φ^y, k_φ^u, k_φ^v, and k_φ^w ($\varphi = x_0, x_1, y_0, y_1$), respectively. For instance, the free boundary can be easily generated by setting the spring stiffness values into zero, and the stiffness values are set to infinite (a larger number, 10^{15} N/m) to achieve a clamped boundary restraint. On the other hand, for the elastic foundations, K_W and K_S are denoted as linear Winkler foundation and Pasternak foundation coefficients, respectively.

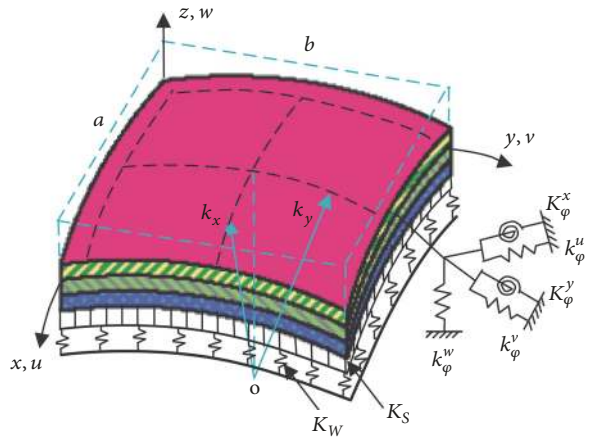

Figure 1: Boundary restraints, linear Winkler and Pasternak foundation for a FGSSS.

In this analysis, different curvature types of FGSSS models, namely, plate ($R_x = R_y = R_{xy} = \infty$), circular cylindrical shell ($R_x = R$, $R_y = R_{xy} = \infty$), spherical shell ($R_x = R_y = R$, $R_{xy} = \infty$), and hyperbolic paraboloidal shell ($R_x = -R_y = R$, $R_{xy} = \infty$), are shown in Figure 2.

Typically, FG layers of shallow shell are made from a mixture of metal and ceramic materials in different proportions. The effective material properties are assumed to vary continuously through the thickness and can be obtained:

$$E(z) = (E_c - E_m) V_c(z) + E_m \tag{2a}$$

$$\rho(z) = (\rho_c - \rho_m) V_c(z) + \rho_m \tag{2b}$$

$$\mu(z) = (\mu_c - \mu_m) V_c(z) + \mu_m \tag{2c}$$

where E, ρ, and μ represent Young's modulus, mass density, and Poisson ratio, respectively, and the subscripts c and m represent the ceramic and metal phase, respectively. $V_c(z)$ is the volume fraction of ceramic constituent. As shown in Figure 3, the representative FGSSS are considered in this work: Type 1 is composed of FG face sheets and homogeneous middle layer (Figure 3(a)); Type 2 has homogeneous face sheets and FG middle layer (Figure 3(b)). $V_c(z)$ of FG sandwich shallow shell in the thickness direction is expressed as

$$\text{Type 1-1: } V_c = \begin{cases} \left(\dfrac{z - z_1}{z_2 - z_1}\right)^{p_1} & z \in [z_1, z_2] \\ 1 & z \in [z_2, z_3] \\ \left(\dfrac{z - z_4}{z_3 - z_4}\right)^{p_3} & z \in [z_3, z_4] \end{cases}$$

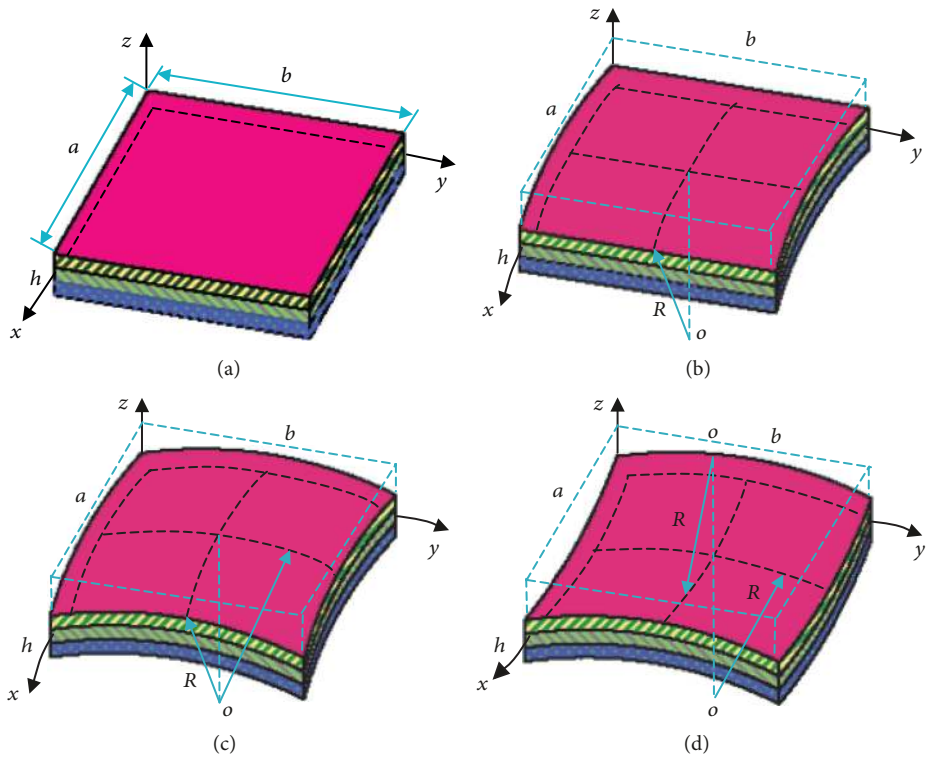

FIGURE 2: Types of curvatures for FGSSS on rectangular planforms: (a) plate; (b) circular cylindrical shell; (c) spherical shell; (d) hyperbolic paraboloidal shell.

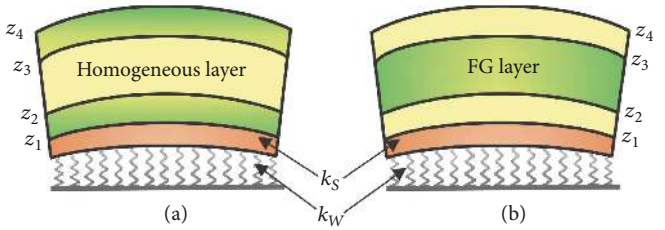

FIGURE 3: The material variation along the thickness of the FGSSS: (a) Type 1: FG face sheets and homogeneous middle layer; (b) Type 2: homogeneous face sheets and FG middle layer.

$$\text{Type 1-2: } V_c = \begin{cases} \left(\dfrac{z - z_1}{z_1 - z_2}\right)^{p_1} & z \in [z_1, z_2] \\ 0 & z \in [z_2, z_3] \\ \left(\dfrac{z - z_3}{z_4 - z_3}\right)^{p_3} & z \in [z_3, z_4] \end{cases} \tag{3a}$$

$$\text{Type 2-1: } V_c = \begin{cases} 1 & z \in [z_1, z_2] \\ \left(\dfrac{z - z_3}{z_2 - z_3}\right)^{p_2} & z \in [z_2, z_3] \\ 0 & z \in [z_3, z_4] \end{cases}$$

$$\text{Type 2-2: } V_c = \begin{cases} 0 & z \in [z_1, z_2] \\ \left(\dfrac{z - z_2}{z_3 - z_2}\right)^{p_2} & z \in [z_2, z_3] \\ 1 & z \in [z_3, z_4] \end{cases} \tag{3b}$$

where the subscripts p_1, p_2, and p_3 are the gradient index used to determine the FG materials and only take nonnegative values. Typical values for metal and ceramic used in the FG layer of shallow shells are listed in Table 1. Type 1-1 and Type 1-2 FGSSS are composed of FG face sheets and

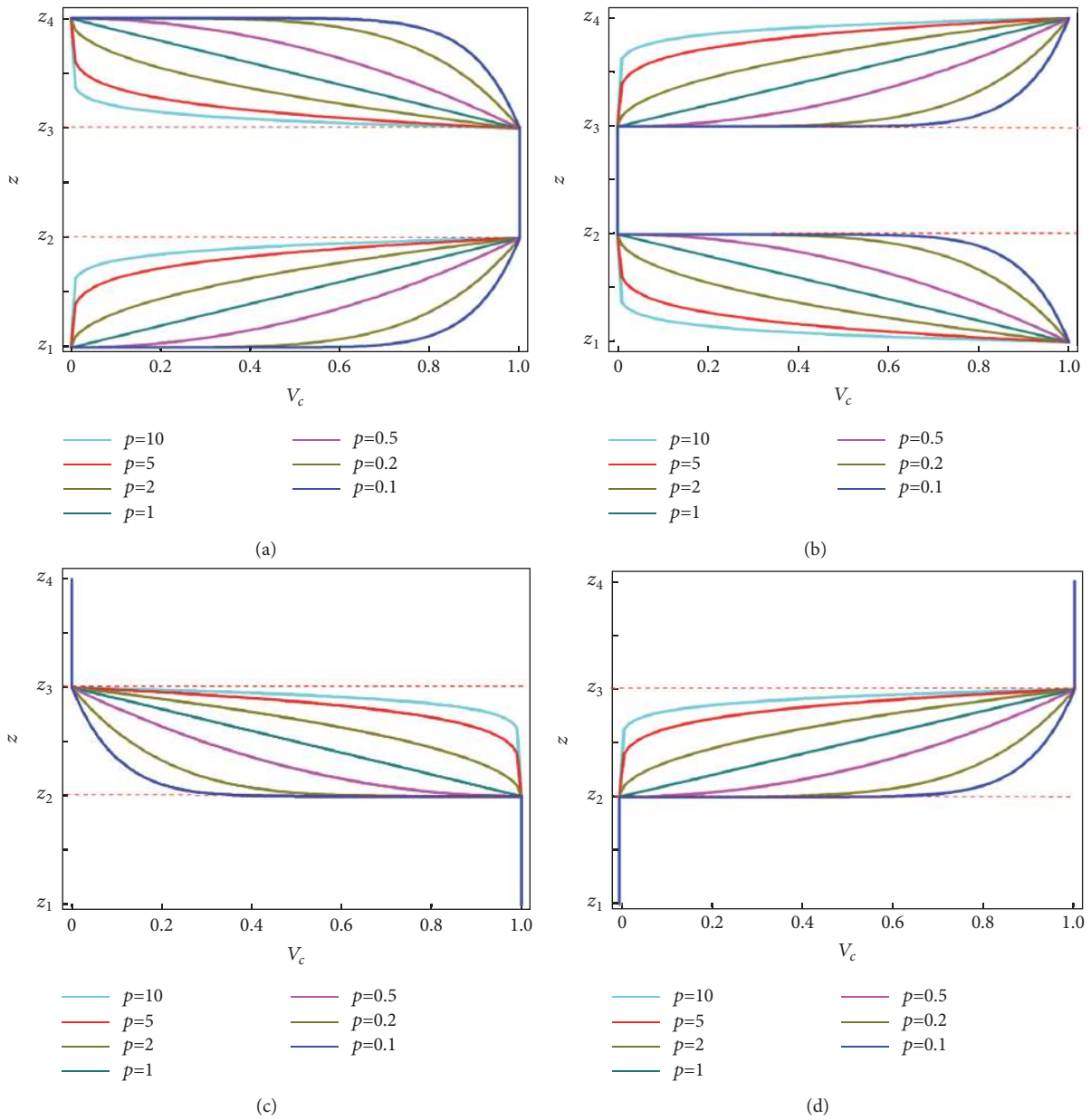

Figure 4: Variation of volume fraction V_c through the thickness in various types: (a) Type 1-1; (b) Type 1-2; (c) Type 2-1; (d) Type 2-2.

homogeneous middle layer, while Type 2-1 and Type 2-2 FGSSS are composed of homogeneous face sheets and FG middle layer. It is found that the bilayered FGSSS can be acquired assigning appropriate ratios of thickness for each layer. And the thickness of each layer from bottom to top is expressed by the combination of three numbers; for instance, "2-3-2" denotes that $h_1 : h_2 : h_3$=2:3:2. To describe the behavior of (3a) and (3b), the volume fractions $V_c(z)$ in the direction of thickness for the FGSSS with various gradient index p are shown in Figure 4.

2.2. Stress-Strain Relations and Stress Resultants. To describe the shell clearly, u, v, and w represent the displacements in the x, y, and z directions, and t is the time variable, respectively.

Table 1: Main materials properties of the used FG layer.

Material	Properties		
	E (GPa)	μ	ρ (kg/m^3)
Metal (Al)	70	0.3	2702
Ceramic (Al_2O_3)	380	0.3	3800

The assumed displacement field for the FGSSS based on the FSDSST can be given by

$$\begin{aligned} U(x, y, z, t) &= u(x, y, t) + z\phi_x(x, y, t) \\ V(x, y, z, t) &= v(x, y, t) + z\phi_y(x, y, t) \\ W(x, y, z, t) &= w(x, y, t) \end{aligned} \tag{4}$$

where ϕ_x and ϕ_y represent the rotations of the reference surface to the y and x axes, respectively. For the FGSSS the strains can be defined as

$$\begin{aligned}\{\varepsilon_x \ \ \varepsilon_y \ \ \gamma_{xy}\}^{\mathrm{T}} &= \left\{\varepsilon_x^0 + z\chi_x \ \ \varepsilon_y^0 + z\chi_y \ \ \gamma_{xy}^0 + z\chi_{xy}\right\}^{\mathrm{T}} \\ &= \left\{\frac{\partial u}{\partial x} \ \ \frac{\partial v}{\partial y} \ \ \frac{\partial u}{\partial y} + \frac{\partial v}{\partial x}\right\}^{\mathrm{T}} \\ &\quad + z\left\{\frac{\partial \phi_x}{\partial x} \ \ \frac{\partial \phi_y}{\partial y} \ \ \frac{\partial \phi_x}{\partial y} + \frac{\partial \phi_y}{\partial x}\right\}^{\mathrm{T}}\end{aligned} \tag{5}$$

$$\begin{aligned}\{\gamma_{xz} \ \ \gamma_{yz}\}^{\mathrm{T}} &= \left\{\gamma_{xz}^0 \ \ \gamma_{yz}^0\right\}^{\mathrm{T}} \\ &= \left\{\frac{\partial u}{\partial z} + \frac{\partial w}{\partial x} \ \ \frac{\partial v}{\partial z} + \frac{\partial w}{\partial y}\right\}^{\mathrm{T}} \\ &= \left\{\phi_x + \frac{\partial w}{\partial x} \ \ \phi_y + \frac{\partial w}{\partial y}\right\}^{\mathrm{T}}\end{aligned} \tag{6}$$

where the normal and shear strains in the directions of x, y, and z are ε_x ε_y and γ_{xy}. γ_{xz} and γ_{yz} are transverse shear strains. According to generalized Hooke's law [46], the stress-strain relations of the shallow shells can be written as

$$\begin{Bmatrix}\sigma_x \\ \sigma_y \\ \tau_{yz} \\ \tau_{xz} \\ \tau_{xy}\end{Bmatrix} = \begin{bmatrix} Q_{11}(z) & Q_{12}(z) & 0 & 0 & Q_{16}(z) \\ Q_{12}(z) & Q_{22}(z) & 0 & 0 & Q_{26}(z) \\ 0 & 0 & Q_{44}(z) & Q_{45}(z) & 0 \\ 0 & 0 & Q_{45}(z) & Q_{55}(z) & 0 \\ Q_{16}(z) & Q_{26}(z) & 0 & 0 & Q_{66}(z)\end{bmatrix} \begin{Bmatrix}\varepsilon_x \\ \varepsilon_y \\ \gamma_{yz} \\ \gamma_{xz} \\ \gamma_{xy}\end{Bmatrix} \tag{7}$$

where the material elastic stiffness coefficients $Q_{ij}(z)$ are defined in terms of the materials properties as

$$\begin{aligned} Q_{11}(z) &= \frac{E(z)}{1-(\mu(z))^2} \\ Q_{44}(z) &= G_{23}(z) \\ Q_{12}(z) &= \frac{E(z)\,\mu(z)}{1-(\mu(z))^2} \\ Q_{55}(z) &= G_{13}(z) \\ Q_{22}(z) &= \frac{E(z)}{1-(\mu(z))^2} \\ Q_{66}(z) &= G_{12}(z) \end{aligned} \tag{8}$$

It should be noted that $G_{12}(z) = G_{13}(z) = G_{23}(z) = E(z)/(2 + 2\mu(z))$. By carrying the integration of stresses over the plate thickness, the force and moment resultants are obtained as

$$\left(N_x, N_y, N_{xy}\right)^{\mathrm{T}} = \int_{-h/2}^{h/2}\left[\sigma_x, \sigma_y, \tau_{xy}\right] dz \tag{9a}$$

$$\left(M_x, M_y, M_{xy}\right)^{\mathrm{T}} = \int_{-h/2}^{h/2}\left[\sigma_x, \sigma_y, \tau_{xy}\right] z\, dz \tag{9b}$$

$$\left(Q_x, Q_y\right)^{\mathrm{T}} = \int_{-h/2}^{h/2}\left[\tau_{xz}, \tau_{yz}\right] dz \tag{9c}$$

where N_x, N_y, N_{xy} are the normal and shear forces, M_x, M_y, and M_{xy} are the bending and twisting moments. Q_x, Q_y are the transverse shear forces. Performing the integration in (9a), (9b), and (9c) yields

$$\begin{aligned}\begin{bmatrix}N_x \\ N_y \\ N_{xy}\end{bmatrix} &= \begin{bmatrix}A_{11} & A_{12} & A_{16} \\ A_{12} & A_{22} & A_{26} \\ A_{16} & A_{26} & A_{66}\end{bmatrix}\left(\frac{\partial u}{\partial x}, \frac{\partial v}{\partial y}, \frac{\partial u}{\partial y} + \frac{\partial v}{\partial x}\right)^{\mathrm{T}} \\ &\quad + \begin{bmatrix}B_{11} & B_{12} & B_{16} \\ B_{12} & B_{22} & B_{26} \\ B_{16} & B_{26} & B_{66}\end{bmatrix}\left(\frac{\partial \phi_x}{\partial x}, \frac{\partial \phi_y}{\partial y}, \frac{\partial \phi_x}{\partial y} + \frac{\partial \phi_y}{\partial x}\right)^{\mathrm{T}}\end{aligned} \tag{10}$$

$$\begin{aligned}\begin{bmatrix}M_x \\ M_y \\ M_{xy}\end{bmatrix} &= \begin{bmatrix}B_{11} & B_{12} & B_{16} \\ B_{12} & B_{22} & B_{26} \\ B_{16} & B_{26} & B_{66}\end{bmatrix}\left(\frac{\partial u}{\partial x}, \frac{\partial v}{\partial y}, \frac{\partial u}{\partial y} + \frac{\partial v}{\partial x}\right)^{\mathrm{T}} \\ &\quad + \begin{bmatrix}D_{11} & D_{12} & D_{16} \\ D_{12} & D_{22} & D_{26} \\ D_{16} & D_{26} & D_{66}\end{bmatrix}\left(\frac{\partial \phi_x}{\partial x}, \frac{\partial \phi_y}{\partial y}, \frac{\partial \phi_x}{\partial y} + \frac{\partial \phi_y}{\partial x}\right)^{\mathrm{T}}\end{aligned} \tag{11}$$

$$\begin{bmatrix}Q_x \\ Q_y\end{bmatrix} = \kappa\begin{bmatrix}A_{44} & A_{45} \\ A_{45} & A_{55}\end{bmatrix}\left(\frac{\partial u}{\partial z} + \frac{\partial w}{\partial x}, \frac{\partial v}{\partial z} + \frac{\partial w}{\partial y}\right)^{\mathrm{T}} \tag{12}$$

where κ denotes the shear correction coefficient and is usually taken as 5/6. The stiffness coefficients A_{ij}, B_{ij}, and D_{ij} can be obtained as

$$\left\{A_{ij}, B_{ij}, D_{ij}\right\} = \sum_{k=1}^{3}\int_{z_k}^{z_{k+1}} Q_{ij}^{(k)}\left\{1, z, z^2\right\} dz \tag{13}$$

2.3. Energy Functions and Governing Equations. A modified Fourier version based on Rayleigh-Ritz method is performed. The Rayleigh-Ritz method is a powerful tool in the field of vibration analysis, in which the undetermined coefficients

in the displacement can be obtained by minimizing the Lagrangian energy function expression or making them equal to zero [47]. Then, a series of equations can be summed up in matrix form as a standard characteristic equation, which can be easily solved to obtain the desired frequencies and modes. The Lagrangian energy function of the FGSSS can be written as

$$L = T - U_s - U_{sp} - U_f + W_e \tag{14}$$

The strain energy U_s for the FGSSS during vibration is given in an integral form by

$$U_s = \frac{1}{2}\int_0^a \int_0^b \left\{N_x\varepsilon_x^0 + N_y\varepsilon_y^0 + N_{xy}\gamma_{xy}^0 + M_x\chi_x + M_y\chi_y + M_{xy}\chi_{xy} + Q_x\gamma_{xz}^0 + Q_y\gamma_{yz}^0\right\} dy\,dx \tag{15}$$

Substituting (5), (6), and (10)-(12) into (15), it can be written in terms of displacements and rotations components as

$$\begin{aligned}
U_s &= \frac{1}{2}\int_0^a \int_0^b \left\{A_{11}\left(\frac{\partial u}{\partial x}\right)^2 + A_{22}\left(\frac{\partial v}{\partial y}\right)^2 + \frac{5}{6}A_{44}\left(\phi_x + \frac{\partial w}{\partial x}\right)^2 + \frac{5}{6}A_{55}\left(\phi_y + \frac{\partial w}{\partial y}\right)^2 + A_{66}\left(\frac{\partial u}{\partial y} + \frac{\partial v}{\partial x}\right)^2 + 2A_{12}\left(\frac{\partial u}{\partial x}\right)\left(\frac{\partial v}{\partial y}\right) + 2A_{16}\left[\left(\frac{\partial u}{\partial x}\right)\left(\frac{\partial u}{\partial y}\right) + \left(\frac{\partial u}{\partial x}\right)\left(\frac{\partial v}{\partial x}\right)\right] + 2A_{26}\left[\left(\frac{\partial v}{\partial x}\right)\left(\frac{\partial v}{\partial y}\right) + \left(\frac{\partial u}{\partial y}\right)\left(\frac{\partial v}{\partial y}\right)\right] + \frac{5}{3}\cdot A_{45}\left[\left(\phi_x + \frac{\partial w}{\partial x}\right)\left(\phi_y + \frac{\partial w}{\partial y}\right)\right] + 2B_{11}\left(\frac{\partial u}{\partial x}\right)\cdot\left(\frac{\partial \phi_x}{\partial x}\right) + 2B_{22}\left(\frac{\partial v}{\partial y}\right)\left(\frac{\partial \phi_y}{\partial y}\right) + 2B_{66}\left(\frac{\partial u}{\partial y} + \frac{\partial v}{\partial x}\right)\left(\frac{\partial \phi_x}{\partial y} + \frac{\partial \phi_y}{\partial x}\right) + 2B_{12}\left[\left(\frac{\partial u}{\partial x}\right)\left(\frac{\partial \phi_y}{\partial y}\right) + \left(\frac{\partial v}{\partial y}\right)\left(\frac{\partial \phi_x}{\partial x}\right)\right] + 2B_{16}\left[\left(\frac{\partial u}{\partial x}\right)\left(\frac{\partial \phi_x}{\partial y}\right) + \left(\frac{\partial u}{\partial x}\right)\left(\frac{\partial \phi_y}{\partial x}\right) + \left(\frac{\partial u}{\partial y}\right)\left(\frac{\partial \phi_x}{\partial x}\right) + \left(\frac{\partial v}{\partial x}\right)\left(\frac{\partial \phi_x}{\partial x}\right)\right] + 2B_{26}\left[\left(\frac{\partial v}{\partial y}\right)\left(\frac{\partial \phi_x}{\partial y}\right) + \left(\frac{\partial v}{\partial y}\right)\left(\frac{\partial \phi_y}{\partial x}\right) + \left(\frac{\partial u}{\partial y}\right)\left(\frac{\partial \phi_y}{\partial y}\right) + \left(\frac{\partial v}{\partial x}\right)\left(\frac{\partial \phi_y}{\partial y}\right)\right] + D_{11}\left(\frac{\partial \phi_x}{\partial x}\right)^2 + D_{22}\left(\frac{\partial \phi_y}{\partial y}\right)^2 + D_{66}\left(\frac{\partial \phi_x}{\partial y} + \frac{\partial \phi_y}{\partial x}\right)^2 + 2D_{12}\left(\frac{\partial \phi_x}{\partial x}\right)\left(\frac{\partial \phi_y}{\partial y}\right) + 2D_{16}\left[\left(\frac{\partial \phi_x}{\partial y}\right)\left(\frac{\partial \phi_x}{\partial x}\right) + \left(\frac{\partial \phi_x}{\partial x}\right)\left(\frac{\partial \phi_y}{\partial x}\right)\right] + 2D_{26}\left[\left(\frac{\partial \phi_x}{\partial y}\right)\left(\frac{\partial \phi_y}{\partial y}\right) + \left(\frac{\partial \phi_y}{\partial x}\right)\left(\frac{\partial \phi_y}{\partial y}\right)\right]\right\} dy\,dx
\end{aligned} \tag{16}$$

The kinetic energy T, external work W_e, and deformation strain energy U_{sp} of the FGSSS can be seen in [48]. Additionally, the strain energy based on the Winkler and Pasternak foundations is

$$U_f = \frac{1}{2}\int_0^a \int_0^b \left\{k_W w^2 + k_S\left(\frac{\partial w}{\partial x}\right)^2 + k_S\left(\frac{\partial w}{\partial y}\right)^2\right\} dy\,dx \tag{17}$$

The governing equations for the FGSSS can be written in matrix form by combining (5), (6), and (10)-(12) based on Hamilton's principle:

$$\left(\begin{bmatrix} L_{11} & L_{12} & L_{13} & L_{14} & L_{15} \\ L_{12} & L_{22} & L_{23} & L_{24} & L_{25} \\ -L_{13} & -L_{23} & L_{33} & L_{34} & L_{35} \\ L_{14} & L_{24} & -L_{34} & L_{44} & L_{45} \\ L_{15} & L_{25} & -L_{35} & L_{45} & L_{55} \end{bmatrix} - w^2\begin{bmatrix} -I_0 & 0 & 0 & -I_1 & 0 \\ 0 & -I_0 & 0 & 0 & -I_1 \\ 0 & 0 & -I_0 & 0 & 0 \\ -I_1 & 0 & 0 & -I_2 & 0 \\ 0 & -I_1 & 0 & 0 & -I_2 \end{bmatrix}\right)\begin{bmatrix} u \\ v \\ w \\ \phi_x \\ \phi_y \end{bmatrix} = \begin{bmatrix} -p_x \\ -p_y \\ -p_z \\ -m_x \\ -m_y \end{bmatrix} \tag{18}$$

The coefficients of the linear operator L_{ij} are given in Appendix A.

2.4. Admissible Displacement Functions. In this subsection, the free vibration of FGSSS on the Winkler and Pasternak foundation with general boundary restraints are considered. The displacement and rotation components of FGSSS consisted of standard double Fourier cosine series and several closed-form supplementary functions are introduced to

remove the potential jumps and boundary discontinuities, which can be expressed as

$$u(x,y,t) = \left\{ \sum_{m=0}^{M}\sum_{n=0}^{N} A_{mn}\cos\lambda_m x\cos\lambda_n y + \sum_{l=1}^{2}\sum_{n=0}^{N} a_l^n \zeta_l^a(x)\cos\lambda_n y + \sum_{l=1}^{2}\sum_{m=0}^{M} b_l^m \zeta_l^b(y)\cos\lambda_m x \right\} e^{i\omega t} \quad (19)$$

$$v(x,y) = \left\{ \sum_{m=0}^{M}\sum_{n=0}^{N} B_{mn}\cos\lambda_m x\cos\lambda_n y + \sum_{l=1}^{2}\sum_{n=0}^{N} c_l^n \zeta_l^a(x)\cos\lambda_n y + \sum_{l=1}^{2}\sum_{m=0}^{M} d_l^m \zeta_l^b(y)\cos\lambda_m x \right\} e^{i\omega t} \quad (20)$$

$$w(x,y,t) = \left\{ \sum_{m=0}^{M}\sum_{n=0}^{N} C_{mn}\cos\lambda_m x\cos\lambda_n y + \sum_{l=1}^{2}\sum_{n=0}^{N} e_l^n \zeta_l^a(x)\cos\lambda_n y + \sum_{l=1}^{2}\sum_{m=0}^{M} f_l^m \zeta_l^b(y)\cos\lambda_m x \right\} e^{i\omega t} \quad (21)$$

$$\phi_x(x,y) = \left\{ \sum_{m=0}^{M}\sum_{n=0}^{N} D_{mn}\cos\lambda_m x\cos\lambda_n y + \sum_{l=1}^{2}\sum_{n=0}^{N} g_l^n \zeta_l^a(x)\cos\lambda_n y + \sum_{l=1}^{2}\sum_{m=0}^{M} h_l^m \zeta_l^b(y)\cos\lambda_m x \right\} e^{i\omega t} \quad (22)$$

$$\phi_y(x,y) = \left\{ \sum_{m=0}^{M}\sum_{n=0}^{N} E_{mn}\cos\lambda_m x\cos\lambda_n y + \sum_{l=1}^{2}\sum_{n=0}^{N} i_l^n \zeta_l^a(x)\cos\lambda_n y + \sum_{l=1}^{2}\sum_{m=0}^{M} j_l^m \zeta_l^b(y)\cos\lambda_m x \right\} e^{i\omega t} \quad (23)$$

where $\lambda_m = m\pi/a$, $\lambda_n = n\pi/b$. M and N are truncation numbers with respect to variables x and y. A_{mn}, B_{mn}, C_{mn}, D_{mn}, and E_{mn} represent the Fourier expansion coefficients of the cosine Fourier series, respectively. a_l^n, b_l^m, c_l^n, d_l^m, e_l^n, f_l^m, g_l^n, h_l^m, i_l^n, and j_l^m are the corresponding supplement coefficients. The auxiliary polynomial functions $\zeta_l^a(x)$ and $\zeta_l^b(y)$ are introduced to remove all the potential discontinuities associated with the first-order derivatives at the boundaries, which can be expressed as follows:

$$\begin{aligned} \zeta_1^a(x) &= x\left(\frac{x}{a}-1\right)^2 \\ \zeta_2^a(x) &= \frac{x^2}{a}\left(\frac{x}{a}-1\right) \\ \zeta_1^b(y) &= y\left(\frac{y}{b}-1\right)^2 \\ \zeta_2^b(y) &= \frac{y^2}{b}\left(\frac{y}{b}-1\right) \end{aligned} \quad (24)$$

It can be verified that

$$\begin{aligned} &\zeta_1^{a'}(0) = 1, \\ &\zeta_1^a(0) = \zeta_1^a(a) = \zeta_1^{a'}(a) = 0 \\ &\zeta_2^{a'}(a) = 1, \\ &\zeta_2^a(0) = \zeta_2^a(a) = \zeta_2^{a'}(0) = 0 \\ &\zeta_1^{b'}(0) = 1, \\ &\zeta_1^b(0) = \zeta_1^b(b) = \zeta_1^{b'}(b) = 0 \\ &\zeta_2^{b'}(b) = 1, \\ &\zeta_2^b(0) = \zeta_2^b(b) = \zeta_2^{b'}(0) = 0 \end{aligned} \quad (25)$$

Alternately, all the expansion coefficients in (19)-(23) are treated equally and independently as the orthogonal coordinates and solved from the Rayleigh-Ritz method. The vibration characteristic equation can be summed up:

$$\left(\mathbf{K} - \omega^2\mathbf{M}\right)\mathbf{G} = 0 \quad (26)$$

where the coefficient eigenvector $\mathbf{G} = [\mathbf{G}^u, \mathbf{G}^v, \mathbf{G}^w, \mathbf{G}^{\phi_x}, \mathbf{G}^{\phi_y}]^{\mathrm{T}}$ is the unknown expansion coefficient that appears in the series expansions and can be determined by

$$\begin{aligned} \mathbf{G}^u &= \left[A_{00}, A_{01}, \cdots, A_{m0}, A_{m1}, \cdots A_{mn}, \cdots, A_{MN}, a_1^0, \cdots, a_l^n, \cdots, a_2^N, b_1^0, \cdots, b_l^m, \cdots, b_2^M\right] \\ \mathbf{G}^v &= \left[B_{00}, B_{01}, \cdots, B_{m0}, B_{m1}, \cdots B_{mn}, \cdots, B_{MN}, c_1^0, \cdots, c_l^n, \cdots, c_2^N, d_1^0, \cdots, d_l^m, \cdots, d_2^M\right] \\ \mathbf{G}^w &= \left[C_{00}, C_{01}, \cdots, C_{m0}, C_{m1}, \cdots C_{mn}, \cdots, C_{MN}, e_1^0, \cdots, e_l^n, \cdots, e_2^N, f_1^0, \cdots, f_l^m, \cdots, f_2^M\right] \end{aligned}$$

Table 2: The corresponding elastic restraint parameters for various boundaries.

Boundary type	Restraint parameters
F	$k_{x_0}^u = k_{x_0}^v = k_{x_0}^w = K_{x_0}^x = K_{x_0}^y = 0,\ N_x = N_{xy} = Q_x = M_x = M_{xy} = 0$
C	$k_{x_0}^u = k_{x_0}^v = k_{x_0}^w = K_{x_0}^x = K_{x_0}^y = 10^7 D,\ u = v = w = \phi_x = \phi_y = 0$
S	$k_{x_0}^u = k_{x_0}^v = k_{x_0}^w = K_{x_0}^y = 10^7 D,\quad K_{x_0}^x = 0,\ u = v = w = M_x = \phi_y = 0$
SD	$k_{x_0}^v = k_{x_0}^w = K_{x_0}^y = 10^7 D,\ k_{x_0}^u = K_{x_0}^x = 0$
E^1	$k_{x_0}^w = K_{x_0}^x = K_{x_0}^y = 10^7 D,\ k_{x_0}^u = k_{x_0}^v = 15D,\ w = \phi_x = \phi_y = 0, u \neq 0, v \neq 0$
E^2	$k_{x_0}^u = k_{x_0}^v = K_{x_0}^x = K_{x_0}^y = 10^7 D,\ k_{x_0}^w = 10D,\ u = v = \phi_x = \phi_y = 0, w \neq 0$
E^3	$k_{x_0}^u = k_{x_0}^v = k_{x_0}^w = 10^7 D,\ K_{x_0}^x = K_{x_0}^y = 5D, u = v = w = 0,\ \phi_x \neq 0,\ \phi_y \neq 0$

Table 3: Comparison of non-dimensional frequency parameters $\varpi = \omega b^2/h\sqrt{\rho_m/E_m}$ of simply supported square FG sandwich plates with homogeneous middle layer.

h/a	p	Theory	ϖ					
			1-0-1	1-1-1	1-2-1	2-1-2	2-2-1	1-8-1
0.01	0.5	3D [42]	1.48244	1.56046	1.61915	1.52355	1.59031	1.76357
		RPT [43]	1.48241	1.56042	1.61912	1.52353	1.59030	1.76354
		Present	1.48248	1.56023	1.61913	1.52358	1.59034	1.76359
	5	3D [42]	0.96563	1.06309	1.19699	0.99903	1.13020	1.56988
		RPT [43]	0.96564	1.06309	1.19697	0.99903	1.13019	1.56985
		Present	0.96566	1.06313	1.19697	0.99907	1.13024	1.56980
	10	3D [42]	0.95042	1.01237	1.14408	0.95934	1.08065	1.54164
		RPT [43]	0.95044	1.01236	1.14406	0.95937	1.08065	1.54162
		Present	0.95041	1.01234	1.14408	0.95935	1.08065	1.54166
0.1	0.5	3D [42]	1.44614	1.52131	1.57668	1.48608	1.54926	1.71130
		RPT [43]	1.44423	1.51921	1.57450	1.48408	1.54710	1.70901
		Present	1.44485	1.51975	1.57461	1.48415	1.54750	1.70920
	5	3D [42]	0.94476	1.04532	1.17567	0.98103	1.10983	1.52993
		RPT [43]	0.94598	1.04465	1.17396	0.98184	1.10881	1.52792
		Present	0.94552	1.04434	1.17355	0.98142	1.10874	1.52805
	10	3D [42]	0.92727	0.99523	1.12466	0.94078	1.06104	1.50333
		RPT [43]	0.92838	0.99550	1.12313	0.94296	1.06090	1.50138
		Present	0.92836	0.99550	1.12313	0.94295	1.06080	1.50137
0.2	0.5	3D [42]	1.35358	1.42178	1.46940	1.39053	1.44535	1.58186
		RPT [43]	1.34743	1.41508	1.46251	1.38410	1.43843	1.57476
		Present	1.35015	1.41682	1.46368	1.38515	1.43901	1.57592
	5	3D [42]	0.89086	0.99798	1.11900	0.93362	1.05607	1.42845
		RPT [43]	0.89462	0.99545	1.11318	0.93594	1.05228	1.42197
		Present	0.89504	0.99561	1.11285	0.93480	1.05496	1.42372
	10	3D [42]	0.86833	0.94984	1.07290	0.89228	1.00949	1.40568
		RPT [43]	0.87178	0.95033	1.06754	0.89918	1.00848	1.39932
		Present	0.86963	0.95012	1.06950	0.89541	1.00887	1.40105

Table 4: Comparisons of nondimensional frequency parameters $\varpi = \omega b^2/h\sqrt{\rho_0/E_0}$ for Type 1-1 and FGSSS with completely free boundary restraints, respectively (a=b, h/b=0.1, and R_{xy}=∞).

Mode	a/R=0.2						a/R=0.5					
	12×12		13 ×13		14×14		12×12		13×13		14×14	
	Jin et al. [44]	Present	Jin et al. [44]	Present	Jin et al. [44]	Present	Jin et al. [44]	Present	Jin et al. [44]	Present	Jin et al. [44]	Present
Type 1-1: FG circular cylindrical shallow shell												
1	0.903	0.907	0.902	0.905	0.902	0.905	0.901	0.903	0.901	0.902	0.901	0.902
2	1.352	1.361	1.352	1.359	1.352	1.358	1.405	1.411	1.405	1.411	1.405	1.410
3	1.662	1.670	1.662	1.666	1.662	1.659	1.734	1.738	1.734	1.735	1.734	1.735
4	2.279	2.285	2.278	2.281	2.278	2.281	2.272	2.275	2.271	2.276	2.271	2.276
Type 1-1: FG spherical shallow shell												
1	0.902	0.905	0.902	0.905	0.902	0.902	0.899	0.904	0.898	0.901	0.898	0.897
2	1.335	1.336	1.335	1.336	1.335	2.334	1.322	1.325	1.322	1.325	1.322	1.325
3	1.696	1.691	1.696	1.694	1.696	1.695	1.900	1.905	1.900	1.905	1.900	1.905
4	2.279	2.284	2.279	2.284	2.279	2.284	2.274	2.276	2.274	2.275	2.274	2.275
Type 1-1: FG hyperbolic paraboloidal shallow shell												
1	0.902	0.905	0.902	0.905	0.902	0.905	0.899	0.896	0.899	0.894	0.899	0.894
2	1.399	1.395	1.399	1.395	1.399	1.394	1.634	1.635	1.634	1.637	1.634	1.638
3	1.648	1.645	1.648	1.645	1.648	1.654	1.683	1.687	1.683	1.687	1.683	1.687
4	2.283	2.285	2.282	2.286	2.282	2.286	2.294	2.296	2.293	2.296	2.293	2.297
Type 2-1: FG circular cylindrical shallow shell												
1	0.835	0.845	0.835	0.845	0.835	0.844	0.833	0.835	0.833	0.834	0.833	0.834
2	1.249	1.245	1.249	1.245	1.249	1.245	1.302	1.306	1.302	1.308	1.302	1.308
3	1.537	1.550	1.537	1.552	1.537	1.553	1.604	1.612	1.604	1.610	1.604	1.610
4	2.105	2.110	2.105	2.110	2.104	2.108	2.104	2.107	2.104	2.107	2.104	2.109
Type 2-1: FG spherical shallow shell												
1	0.835	0.838	0.834	0.835	0.834	0.832	0.830	0.834	0.830	0.835	0.830	0.835
2	1.235	1.241	1.235	1.239	1.235	1.238	1.227	1.231	1.227	1.234	1.227	1.234
3	1.570	1.574	1.570	1.574	1.570	1.574	1.765	1.768	1.765	1.767	1.764	1.767
4	2.106	2.110	2.105	2.110	2.105	2.108	2.105	2.109	2.105	2.114	2.105	2.114
Type 2-1: FG hyperbolic paraboloidal shallow shell												
1	0.836	0.841	0.835	0.838	0.835	0.837	0.832	0.835	0.832	0.836	0.832	0.836
2	1.291	1.294	1.291	1.294	1.291	1.294	1.507	1.521	1.507	1.521	1.507	1.520
3	1.522	1.532	1.522	1.537	1.522	1.540	1.555	1.547	1.555	1.549	1.555	1.551
4	2.101	2.104	2.101	2.114	2.104	2.107	2.106	2.115	2.105	2.114	2.105	2.114

$$\mathbf{G}^{\phi_x} = \left[D_{00}, D_{01}, \cdots, D_{m0}, D_{m1}, \cdots D_{mn}, \cdots, D_{MN}, g_1^0, \cdots, g_l^n, \cdots, g_2^N, h_1^0, \cdots, h_l^m, \cdots, h_2^M\right]$$

$$\mathbf{G}^{\phi_y} = \left[E_{00}, E_{01}, \cdots, E_{m0}, E_{m1}, \cdots E_{mn}, \cdots, E_{MN}, i_1^0, \cdots, i_l^n, \cdots, i_2^N, j_1^0, \cdots, j_l^m, \cdots, j_2^M\right] \quad (27)$$

$\mathbf{K}$ and $\mathbf{M}$ represent the stiffness and mass matrix of the FGSSS, respectively. Both of them are matrices and can be expressed as [48]

$$\mathbf{K} = \begin{bmatrix} \mathbf{K}_{uu} & \mathbf{K}_{uv} & \mathbf{K}_{uw} & \mathbf{K}_{u\phi_x} & \mathbf{K}_{u\phi_y} \\ \mathbf{K}_{uv} & \mathbf{K}_{vv} & \mathbf{K}_{vw} & \mathbf{K}_{v\phi_x} & \mathbf{K}_{v\phi_y} \\ \mathbf{K}_{uw} & \mathbf{K}_{vw} & \mathbf{K}_{ww} & \mathbf{K}_{w\phi_x} & \mathbf{K}_{w\phi_y} \\ \mathbf{K}_{u\phi_x} & \mathbf{K}_{v\phi_x} & \mathbf{K}_{w\phi_x} & \mathbf{K}_{\phi_x\phi_x} & \mathbf{K}_{\phi_x\phi_y} \\ \mathbf{K}_{u\phi_y} & \mathbf{K}_{v\phi_y} & \mathbf{K}_{w\phi_y} & \mathbf{K}_{\phi_x\phi_y} & \mathbf{K}_{\phi_y\phi_y} \end{bmatrix}$$

Table 5: The first four frequencies f (Hz) for Type 1-1 (1-1-1) FGSSS with various boundary restraints and radius-length ratios (p=5, a/b=1, and h/a=0.1).

R_x/R_y	R_x/a	Mode	Boundary restraints							
			SSSS	CCCC	CFCF	SCSC	CSDCSD	$CE^1E^1E^1$	SE^2SE^2	$E^3E^3E^3E^3$
Plate	∞	1	66.545	79.857	72.148	58.102	75.279	39.310	74.196	21.214
		2	93.851	105.51	96.792	73.858	99.082	51.903	98.154	35.150
		3	138.47	140.48	123.95	97.593	123.27	71.192	102.21	45.211
		4	159.68	173.65	143.54	120.97	135.36	98.115	125.34	59.633
+1	5	1	68.563	80.374	75.156	60.154	78.364	40.151	77.458	23.157
		2	97.471	106.35	85.215	79.585	95.544	53.31	90.17	41.405
		3	135.54	133.37	98.410	89.361	126.55	79.87	107.01	58.649
		4	152.12	159.51	112.12	103.52	135.10	108.81	130.97	61.056
	2	1	76.167	87.355	78.124	72.195	83.954	43.486	80.853	25.699
		2	90.544	106.05	95.439	80.398	97.610	55.439	98.398	46.378
		3	99.202	117.08	106.25	97.403	116.21	86.925	107.403	71.642
		4	119.14	139.52	115.58	115.46	130.47	100.54	125.468	76.557
0	5	1	64.479	78.545	67.191	58.235	74.407	36.419	70.435	21.244
		2	89.655	96.405	85.366	78.981	89.541	55.661	98.918	45.112
		3	105.24	120.94	109.01	99.210	111.24	79.015	119.21	55.880
		4	126.50	135.79	122.47	119.58	125.19	95.471	139.58	73.385
	2	1	70.571	82.998	73.164	64.771	79.547	39.486	75.761	23.446
		2	86.454	89.699	89.101	82.913	85.254	58.212	93.157	47.254
		3	102.15	117.20	117.80	100.24	100.30	82.172	109.97	60.351
		4	105.85	126.79	128.58	115.38	123.21	90.309	110.58	76.245
-1	5	1	56.152	69.385	59.526	51.402	65.265	32.863	61.626	20.137
		2	79.544	89.510	69.624	77.273	84.541	59.784	76.587	37.560
		3	100.58	111.34	85.060	94.783	100.24	80.479	92.129	54.783
		4	126.24	130.75	115.11	109.23	135.97	92.442	127.66	57.311
	2	1	65.931	79.312	68.214	60.109	75.542	38.651	70.721	22.192
		2	79.654	95.702	85.824	82.562	89.032	60.082	95.104	45.595
		3	98.312	123.54	103.96	95.351	112.33	79.364	107.31	53.102
		4	105.29	126.50	120.54	100.33	135.61	87.115	120.25	69.548

$$\mathbf{M} = \begin{bmatrix} \mathbf{M}_{uu} & \mathbf{0} & \mathbf{0} & \mathbf{M}_{u\phi_x} & \mathbf{0} \\ \mathbf{0} & \mathbf{M}_{uu} & \mathbf{0} & \mathbf{0} & \mathbf{M}_{v\phi_y} \\ \mathbf{0} & \mathbf{0} & \mathbf{M}_{ww} & \mathbf{0} & \mathbf{0} \\ \mathbf{M}_{u\phi_x} & \mathbf{0} & \mathbf{0} & \mathbf{M}_{\phi_x\phi_x} & \mathbf{0} \\ \mathbf{0} & \mathbf{M}_{v\phi_y} & \mathbf{0} & \mathbf{0} & \mathbf{M}_{\phi_y\phi_y} \end{bmatrix} \tag{28}$$

The stiffness matrix **K** and mass matrix **M** are given in Appendix B.

3. Numerous Results and Discussion

In this section, a comprehensive free vibration analysis for FGSSS on Winkler and Pasternak foundations with general boundary restraints is presented. Firstly, the current results are checked by comparing with those results published in other literature. Then, the vibration behaviors for FGSSS on Winkler and Pasternak foundations with various curvature types, distribution types, geometrical parameters, and boundary restraints are studied. Finally, the influence of vibration parameters including inertia, shear deformation, and foundation coefficient on the free vibration is illustrated.

3.1. FGSSS with General Boundary Restraints. In the engineering applications, the letters F, C, S, and SD represent the completely free, completely clamped, simply supported, and shear-diaphragm supported boundary restraints, respectively. Besides the aforementioned classical boundary restraints, three elastic boundary restraints, denoted by E^1, E^2, and E^3, are considered in this paper. Taking edge at x=0, for example, the seven boundaries and corresponding restraint parameters are shown in Table 2.

The reference bending stiffness $D_m = E_m h^3/12(1-\mu_m^2)$. The accuracy and reliability of the current results are displayed in Tables 3 and 4. Table 3 compares the nondimensional frequency parameters $\bar{\omega} = \omega b^2/h\sqrt{\rho_m/E_m}$ of simply

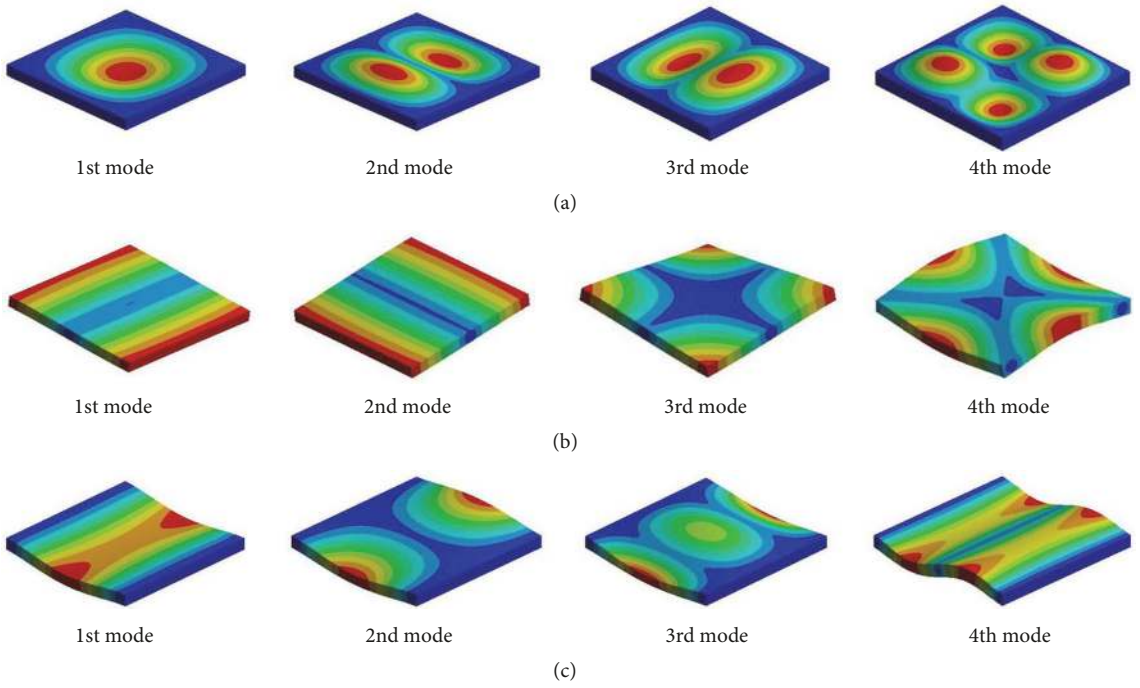

Figure 5: Mode shapes for plates with boundary restraints: (a) CCCC; (b) SSSS; (c) SE^2SE^2.

supported square FG sandwich plates with FG face sheets and homogeneous middle layer (1-0-1, 1-1-1, 1-2-1, 2-1-2, 2-2-1, and 1-8-1). The thickness-length ratios are taken to be h/a=0.01, 0.1, and 0.2. The gradient indexes are given as p=0.5, 5, and 10. Young's modulus, mass density, and Poisson ratio are obtained in Table 1. The solutions given by Li et al. [42], by the 3D solutions and those of Hadji et al. [43], and by the RPT are provided for the comparisons. The differences are less than 1.530% and 2.015% for the worst case, respectively.

Meanwhile, The frequency parameters $\varpi = \omega b^2/h\sqrt{\rho_0/E_0}$ (ρ_0 = 1kg/m^3, E_0 = 1Gpa) for Type 1-1 and Type 2-1 FGSSS with completely free boundary restraints are presented in Table 4. All layers are assumed to be of equal thickness. The geometrical parameters are given as a=b and h/b=0.1. The length-radii ratios used for this analysis are a/R=0.2 and 0.5, and the truncation number is M=N=12, 13, and 14. The frequency results are compared with the solutions given by Jin et al. [44]. A well agreement can be obtained.

Numerous new results for fundamental frequencies f (Hz) are presented in Table 5 for Type 1-1 FGSSS with a variety of general boundary restraints. The gradient index and geometrical parameters are given as p=5, a/b=1, h/a=0.1, R_x/a=2 and 5. And the thickness for each layer is set to be equal. Young's modulus, mass density, and Poisson ratio are showed in Table 1. The boundary restraints including SSSS, CCCC, CFCF, SCSC, CSDCSD, $CE^1E^1E^1$, SE^2SE^2, and $E^3E^3E^3E^3$ are considered. It is obvious that the values of fundamental frequencies corresponding to different boundaries are quite sensitive to the change of geometrical parameters. The frequencies of the FGSSS increase with the increase of radius ratio (R_x/R_y) and the decrease of radius-length ratio (R_x/a). The first four mode shapes for the plate, circular cylindrical shallow shell, and spherical shallow shell with CCCC, SSSS, and SE^2SE^2 boundaries are depicted in Figures 5, 6, and 7, respectively. The radius-length ratio R_x/a is set as 2.

3.2. FGSSS Resting on Winkler and Pasternak Foundations. In this subsection, the free vibration of Type 1-2 (1-1-1) FGSSS on Winkler and Pasternak foundations with general boundary restraints is investigated. The geometric parameters and gradient index of the models are a=b=1 m, h/a=0.1, R_x/a=2, p=0.5 and 5. Winkler coefficient K_W and Pasternak coefficient K_S are taken to be 10 and 100. Young's modulus, mass density, and Poisson ratio of the structures are obtained in Table 1. As known in Table 6, numerous new solutions of fundamental frequencies f (Hz) for the FG sandwich plates, circular cylindrical, spherical, and hyperbolic paraboloidal shallow shells on Winkler and Pasternak foundations with various boundaries (SSSS, CCCC, CFCF, SCSC, CSDCSD, $CE^1E^1E^1$, SE^2SE^2, and $E^3E^3E^3E^3$) are presented. These results can be used as the benchmark solutions for future research in this field. From the results, it is clear that the variation of the Winkler and Pasternak coefficients has the significant effect on frequencies of the shallow shells. In order to further explore the influence of foundation coefficients K_W and K_S on the frequency parameter of the FGSSS, the detailed parametric study will be illustrated in the next subsection.

3.3. Studies on Free Vibration Parameters. In this subsection, the influence of vibration parameters including inertia, shear

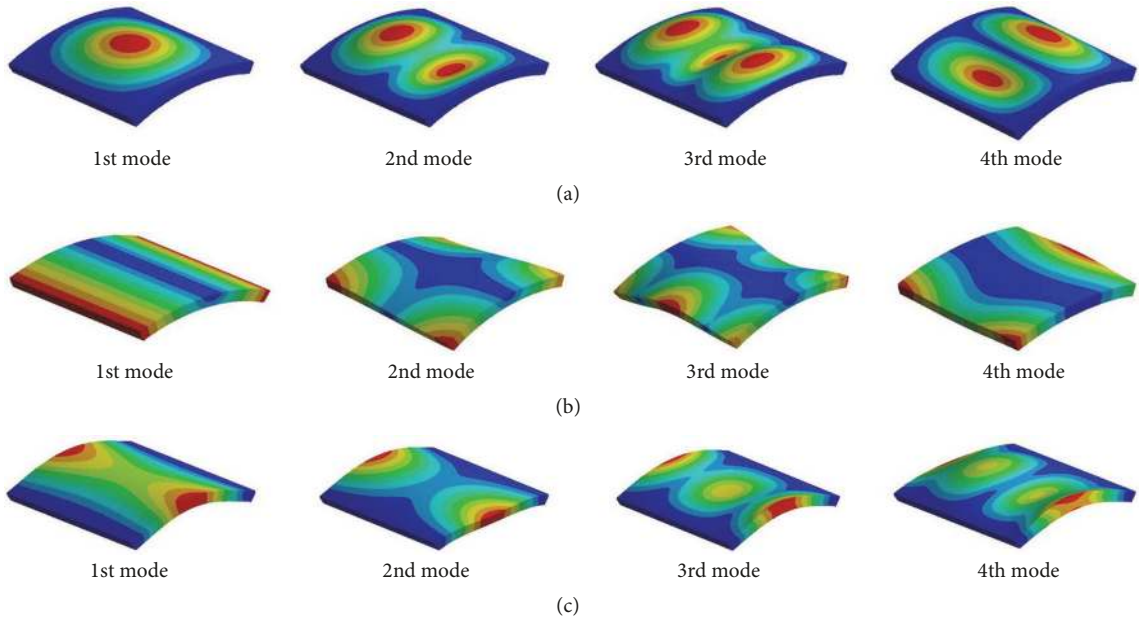

Figure 6: Mode shapes for circular cylindrical shallow shells with boundary restraints: (a) CCCC; (b) SSSS; (c) SE^2SE^2.

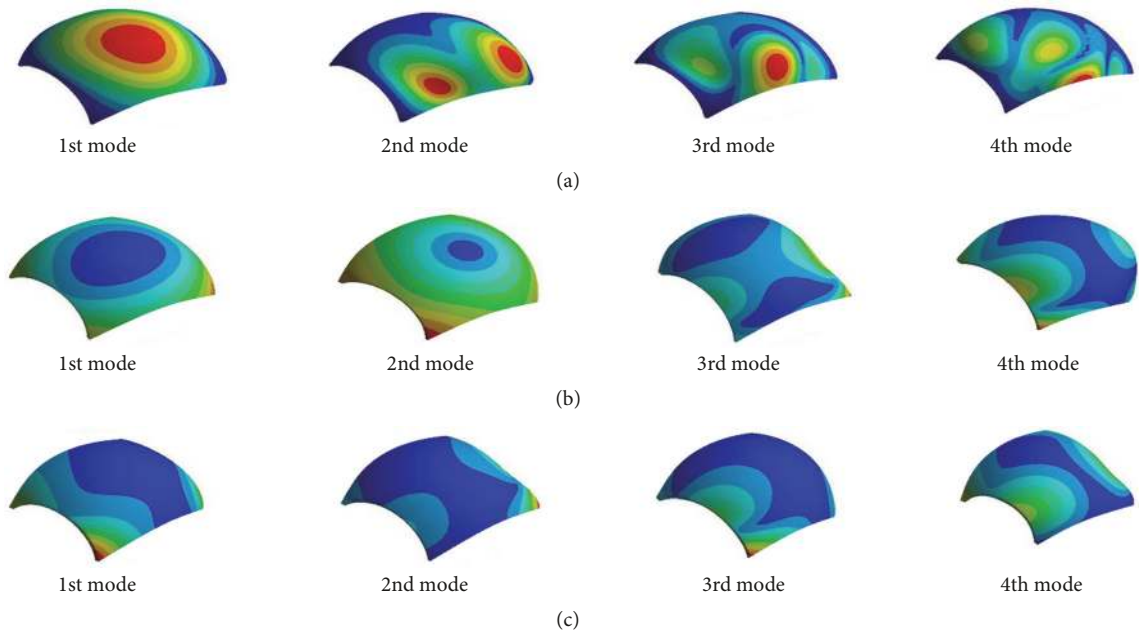

Figure 7: Mode shapes for spherical shallow shells with boundary restraints: (a) CCCC; (b) SSSS; (c) SE^2SE^2.

deformation, and foundation coefficient on the free vibration is illustrated. For CSST, the inertia and shear deformation are not considered in solving the vibration characteristic of FG shallow shells. Consequently, the modified FSDSST is addressed to tackle above problems.

The difference of frequency parameters Ω obtained by CSST and FSDSST for simply supported Type 1-2 FGSSS with various thickness ratios and curvature types is shown in Figure 8. The gradient index and geometric parameters used are p=2, a/b=1, and R_x/a=2. It is clear that the difference of frequency parameters grows with the increase of thickness ratios for all curvature types. Mode shape of (2, 2) displayed larger errors than that of (1, 1), (2, 1), and (1, 2). Hence, CSST is not suitable for the FGSSS due to the important role of inertia and shear deformation in frequency calculation of high-order mode. Furthermore, the difference of frequency

Table 6: Fundamental frequencies f (Hz) for Type 1-2 (1-1-1) plate, circular cylindrical spherical and hyperbolic paraboloidal shallow shell on Winkler and Pasternak foundations with various boundary restraints.

K_W	K_S	ρ	Boundary Restraints							
			SSSS	CCCC	CFCF	SCSC	CSDCSD	$CE^1E^1E^1$	SE^2SE^2	$E^3E^3E^3E^3$
FG sandwich plate										
10	10	0.5	69.151	99.615	89.141	94.136	96.018	43.372	77.252	33.384
		5	58.754	78.703	68.155	72.151	74.712	39.165	62.801	30.728
	100	0.5	77.465	113.40	96.752	102.41	109.86	52.692	84.752	36.832
		5	62.938	92.796	78.234	81.182	88.751	45.648	71.867	31.659
100	10	0.5	78.746	115.76	99.268	105.15	110.21	53.701	84.736	36.685
		5	62.998	95.398	81.680	85.145	91.327	46.408	71.651	30.625
	100	0.5	93.545	131.45	113.04	121.96	128.63	58.310	101.71	38.547
		5	73.742	112.72	80.124	96.584	106.23	52.522	78.087	33.201
FG sandwich circular cylindrical shallow shell										
10	10	0.5	63.850	87.642	78.359	85.209	83.678	40.214	71.065	29.548
		5	54.243	69.245	61.953	69.321	65.251	35.247	56.428	27.651
	100	0.5	70.955	102.96	90.145	94.547	98.932	46.367	75.992	31.287
		5	58.987	93.970	71.625	78.520	90.240	41.140	70.222	29.748
100	10	0.5	72.568	109.64	92.323	98.336	105.63	46.215	80.571	32.214
		5	60.962	94.353	74.254	81.351	89.321	40.162	72.678	28.967
	100	0.5	84.647	125.21	103.35	112.42	118.96	50.271	89.524	35.124
		5	68.166	110.79	78.547	90.244	106.71	45.214	75.215	31.258
FG sandwich spherical shallow shell										
10	10	0.5	54.156	69.759	60.297	64.392	64.253	35.157	58.739	25.172
		5	46.394	57.443	52.061	54.163	52.360	32.658	49.154	22.698
	100	0.5	63.582	95.245	88.570	89.571	93.575	37.687	68.215	26.215
		5	48.151	81.524	70.657	76.408	77.074	34.186	53.216	24.154
100	10	0.5	65.696	102.75	85.041	92.019	98.709	39.398	74.155	26.687
		5	50.168	88.178	70.992	74.326	84.171	35.187	65.397	25.154
	100	0.5	74.963	116.32	95.891	104.45	110.38	44.163	82.357	29.696
		5	67.490	105.88	74.126	85.247	101.49	40.352	70.644	27.215
FG sandwich hyperbolic paraboloidal shallow shell										
10	10	0.5	34.248	43.435	38.423	40.317	40.457	31.971	36.215	22.198
		5	30.157	38.480	34.767	36.051	36.370	28.645	32.367	20.067
	100	0.5	45.955	64.016	54.031	57.309	58.036	34.196	50.397	24.548
		5	39.221	52.482	45.021	46.322	49.467	30.677	42.255	22.001
100	10	0.5	48.251	69.245	60.652	63.567	63.259	35.672	53.219	25.157
		5	38.195	53.522	45.682	49.294	50.245	31.015	41.488	24.695
	100	0.5	50.003	82.795	62.052	68.088	78.590	32.359	58.154	28.964
		5	41.326	72.278	49.992	53.355	66.048	30.248	45.570	26.175

parameters Ω obtained by CSST and FSDSST for simply supported FG spherical shallow shells with different thickness ratios and anisotropic degrees are plotted in Figure 9. It can be seen that the difference of frequency parameters increases with the increase of anisotropic degrees, which suggests that the effect of inertia and shear deformation is magnified when anisotropic degrees are taken to be larger values. However, due to the influence of mode shape and anisotropic degrees, the difference of frequency parameters for some FG spherical shallow shells may show a decreasing trend after reaching a certain thickness ratio. Furthermore, the variations of frequency parameters Ω versus the foundation coefficients for simply supported Type 1-2 (1-1-1) FGSSS are presented in Figure 10. It can be easily obtained that the change in frequencies parameters is very small when the Winkler and Pasternak foundation coefficients are less than 10^5, while when the values of Winkler and Pasternak foundation coefficients are between 10^5 and 10^9, the frequencies

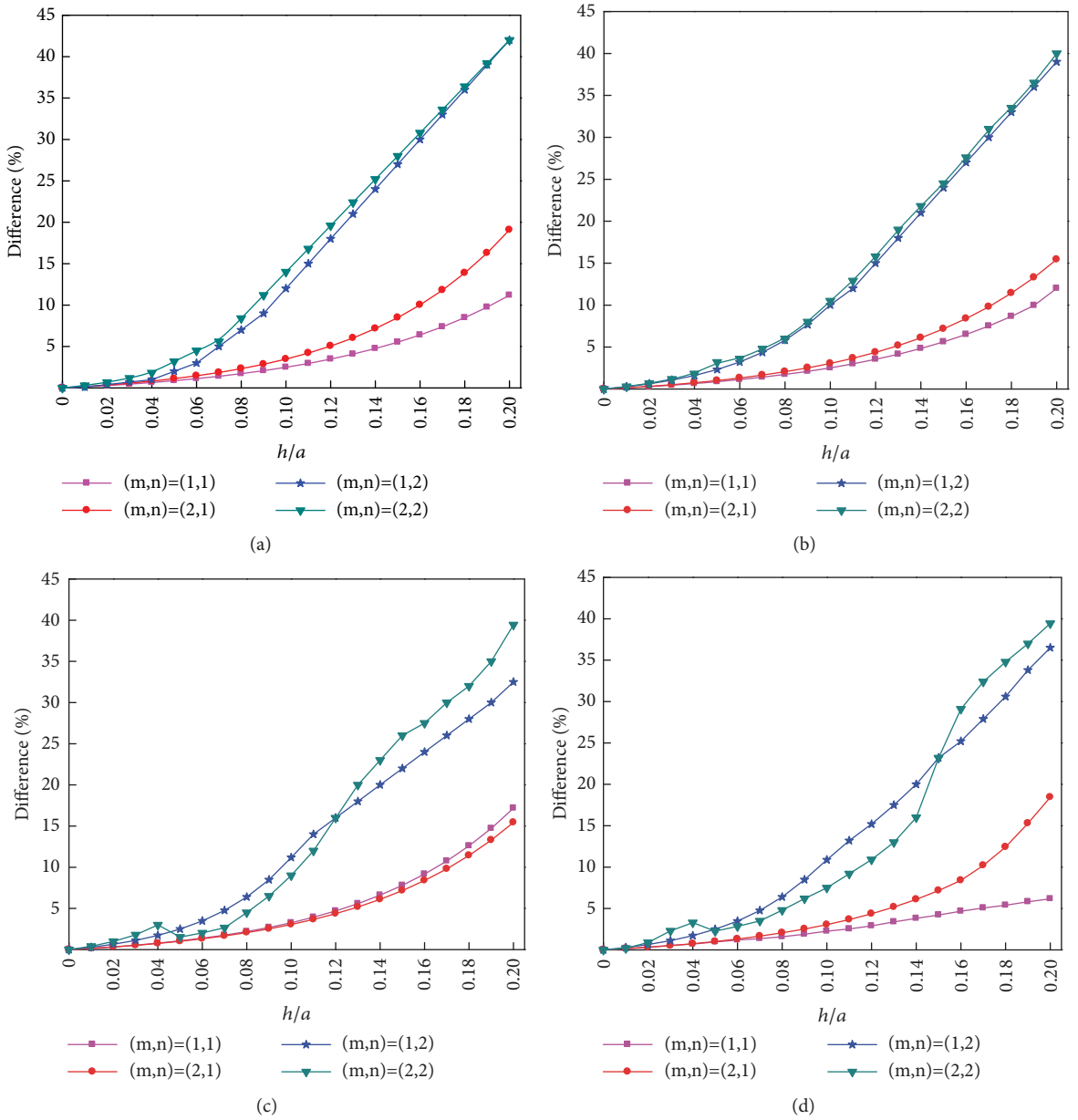

FIGURE 8: The difference of frequency parameters Ω obtained by CSST and FSDSST for simply supported FGSSS with different thickness ratios h/a and curvature types: (a) plate; (b) circular cylindrical shallow shell; (c) spherical shallow shell; (d) hyperbolic paraboloidal shallow shell. (m and n represent the modal number in the direction of x and y, respectively).

parameters increase rapidly, which is a sensitive range. In the case of greater than 10^9, the effect of Winkler and Pasternak foundation coefficients on the frequencies parameters Ω can be neglected.

4. Conclusions

This paper presents a modified Fourier method for free vibration of FGSSS on Winkler and Pasternak foundations based on FSDSST. Vibration characteristics of the shallow shells have been obtained by the energy function represented in the orthogonal coordinates, in which the displacement and rotation components are described as a combining form of standard double Fourier cosine series and several closed-form supplementary functions in order to eliminate the potential jumps and boundary discontinuities. The present method displays better reliability and accuracy. Then, numerous new results for FGSSS on Winkler and Pasternak foundations with various curvature types, geometrical parameters, and boundary restraints are presented, which may be used for benchmark solutions in the future research.

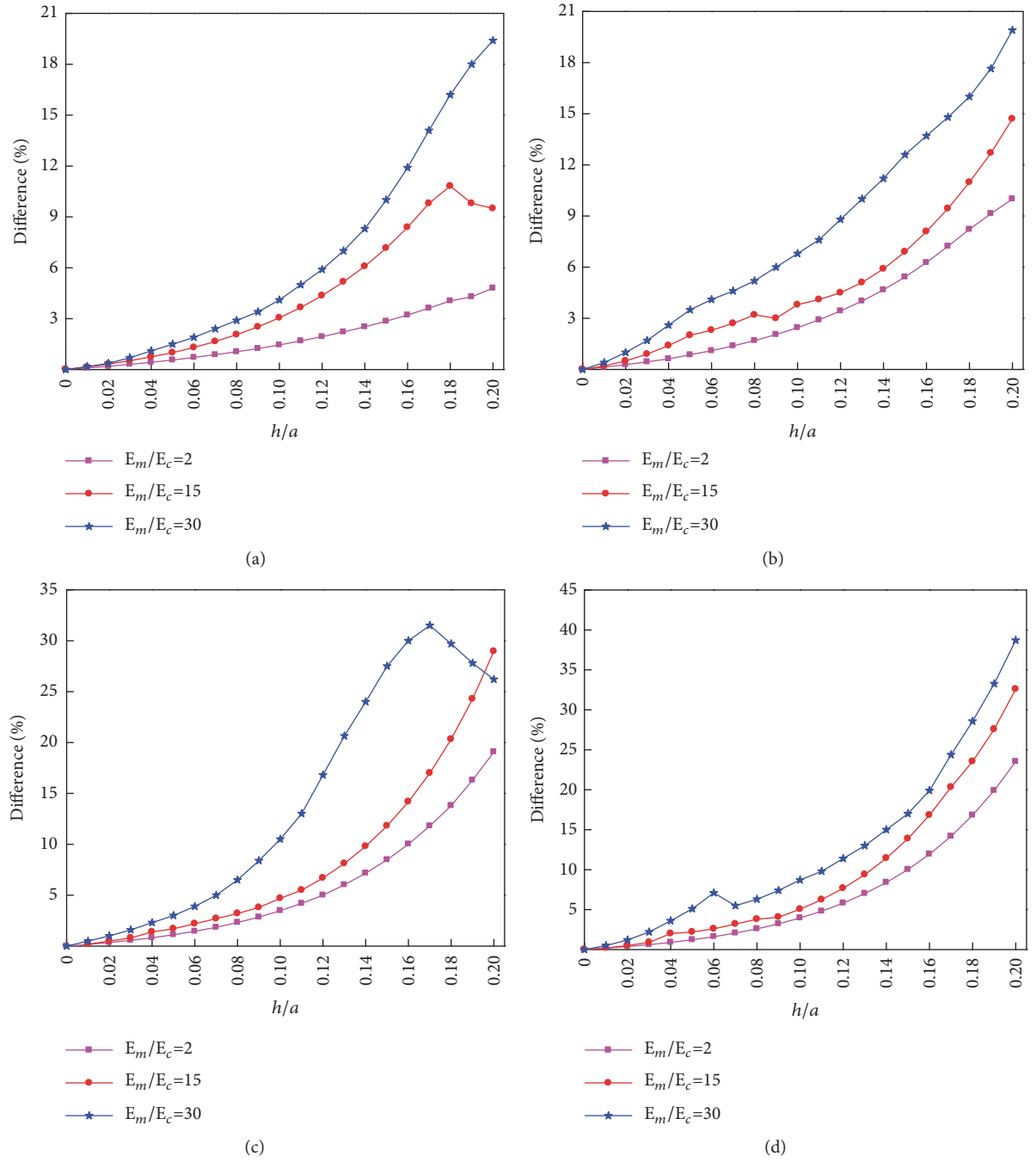

FIGURE 9: The difference of frequency parameters Ω obtained by CSST and FSDSST for simply supported FG spherical shallow shells with different thickness ratios h/a and anisotropic degrees E_m/E_c: (a) (1, 1); (b) (2, 1); (c) (1, 2); (d) (2, 2).

In addition, a comprehensive investigation concentrated on the free vibration characteristics of FGSSS is performed. The results show that the inertia, shear deformation, and foundation coefficients are verified to affect significantly the vibration frequencies of FGSSS. The difference of frequency parameters increases with the increase of anisotropic degrees, which proves that the effect of inertia and shear deformation is magnified when anisotropic degrees are taken to be larger values. And the change in frequencies parameters is small when the Winkler and Pasternak foundation coefficients are less than 10^5, while when the values of Winkler and Pasternak foundation coefficients are between 10^5 and 10^9, the frequencies parameters increase rapidly. In the case of greater than 10^9, the effect of foundation coefficients on the frequencies parameters can be neglected.

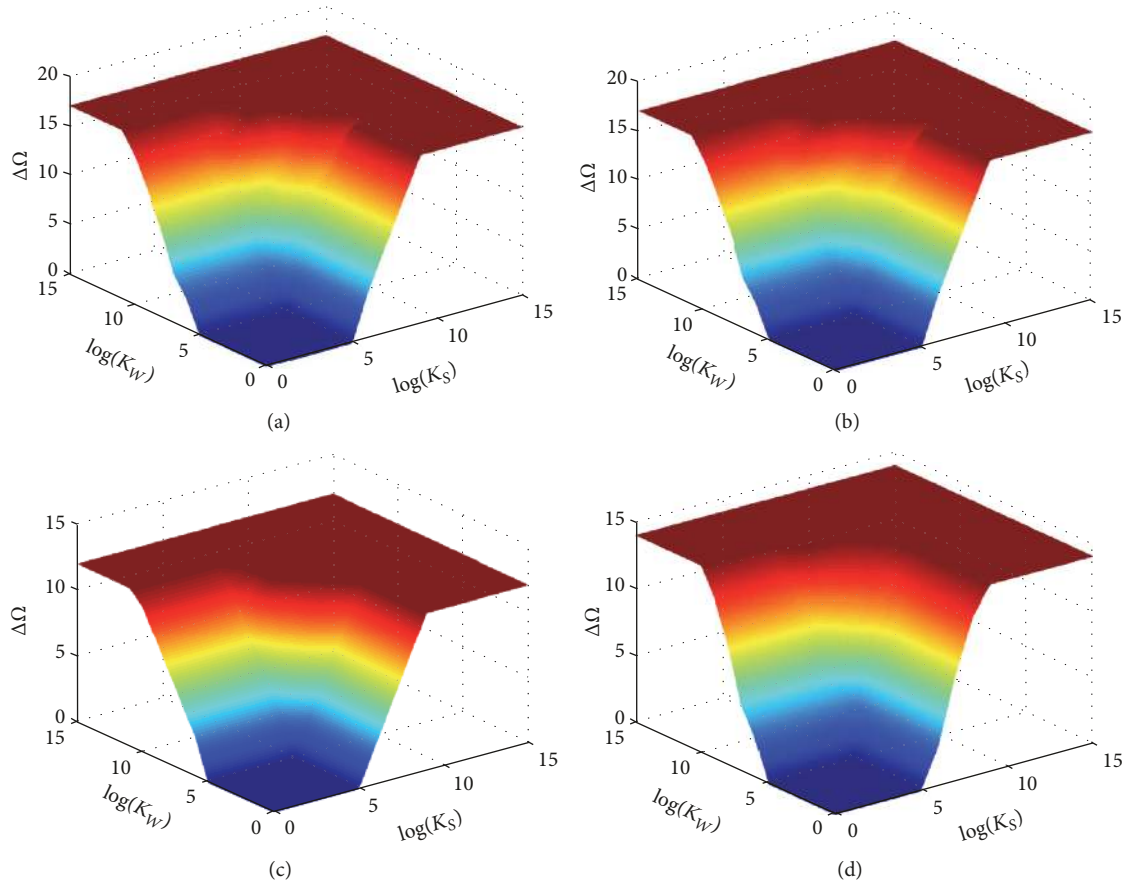

FIGURE 10: Variation of the frequency parameters versus the foundation coefficients for simply supported FGSSS with various curvature types. (a) plate; (b) circular cylindrical shallow shell; (c) spherical shallow shell; (d) hyperbolic paraboloidal shallow shell.

Appendix

A. Linear Differential Operator of the Governing Equation

The coefficients of the linear operator L_{ij} are as follows:

$$L_{11} = A_{11}\frac{\partial^2}{\partial x^2} + 2A_{16}\frac{\partial^2}{\partial x\partial y} + A_{66}\frac{\partial^2}{\partial y^2} - \frac{A_{55}}{R_x^2}$$

$$L_{12} = A_{16}\frac{\partial^2}{\partial x^2} + (A_{12} + A_{66})\frac{\partial^2}{\partial x\partial y} + A_{26}\frac{\partial^2}{\partial y^2} - \frac{A_{45}}{R_xR_y}$$

$$L_{13} = \left(\frac{A_{11}}{R_x} + \frac{A_{12}}{R_y} + \frac{A_{55}}{R_x}\right)\frac{\partial}{\partial x} + \left(\frac{A_{16}}{R_x} + \frac{A_{26}}{R_y} + \frac{A_{45}}{R_x}\right)\frac{\partial}{\partial y}$$

$$L_{14} = B_{11}\frac{\partial^2}{\partial x^2} + 2B_{16}\frac{\partial^2}{\partial x\partial y} + B_{66}\frac{\partial^2}{\partial y^2} + \frac{A_{55}}{R_x}$$

$$L_{15} = B_{16}\frac{\partial^2}{\partial x^2} + (B_{12} + B_{66})\frac{\partial^2}{\partial x\partial y} + B_{26}\frac{\partial^2}{\partial y^2} + \frac{A_{45}}{R_x}$$

$$L_{22} = A_{66}\frac{\partial^2}{\partial x^2} + 2A_{26}\frac{\partial^2}{\partial x\partial y} + A_{22}\frac{\partial^2}{\partial y^2} - \frac{A_{44}}{R_y^2}$$

$$L_{23} = \left(\frac{A_{12}}{R_x} + \frac{A_{22}}{R_y} + \frac{A_{44}}{Ry}\right)\frac{\partial}{\partial y} + \left(\frac{A_{16}}{R_x} + \frac{A_{26}}{R_y} + \frac{A_{45}}{Ry}\right)\frac{\partial}{\partial x}$$

$$L_{24} = B_{16}\frac{\partial^2}{\partial x^2} + (B_{12} + B_{66})\frac{\partial^2}{\partial x\partial y} + B_{26}\frac{\partial^2}{\partial y^2} + \frac{A_{45}}{R_y}$$

$$L_{25} = B_{66}\frac{\partial^2}{\partial x^2} + 2B_{26}\frac{\partial^2}{\partial x\partial y} + B_{22}\frac{\partial^2}{\partial y^2} + \frac{A_{44}}{R_y}$$

$$L_{33} = \frac{A_{11}}{R_x^2} + \frac{2A_{12}}{R_xR_y} + \frac{A_{22}}{R_y^2} - A_{55}\frac{\partial^2}{\partial x^2} - 2A_{45}\frac{\partial^2}{\partial x\partial y} - A_{44}\frac{\partial^2}{\partial y^2} + k_w - k_s\left(\frac{\partial^2}{\partial x^2} + \frac{\partial^2}{\partial y^2}\right)$$

$$
\begin{aligned}
L_{34} &= \left(\frac{B_{11}}{R_x} + \frac{A_{12}}{R_y} - A_{55}\right)\frac{\partial}{\partial x} \\
&\quad + \left(\frac{B_{16}}{R_x} + \frac{B_{26}}{R_y} - A_{45}\right)\frac{\partial}{\partial y} \\
L_{35} &= \left(\frac{B_{12}}{R_x} + \frac{A_{22}}{R_y} - A_{44}\right)\frac{\partial}{\partial y} \\
&\quad + \left(\frac{B_{16}}{R_x} + \frac{B_{26}}{R_y} - A_{45}\right)\frac{\partial}{\partial x} \\
L_{44} &= D_{11}\frac{\partial^2}{\partial x^2} + 2D_{16}\frac{\partial^2}{\partial x \partial y} + D_{66}\frac{\partial^2}{\partial y^2} - A_{55} \\
L_{45} &= D_{16}\frac{\partial^2}{\partial x^2} + (D_{12} + D_{66})\frac{\partial^2}{\partial x \partial y} + D_{26}\frac{\partial^2}{\partial y^2} - A_{45} \\
L_{55} &= D_{66}\frac{\partial^2}{\partial x^2} + 2D_{26}\frac{\partial^2}{\partial x \partial y} + D_{22}\frac{\partial^2}{\partial y^2} - A_{44}
\end{aligned} \tag{A.1}
$$

B. Stiffness and Mass Matrix

Submatrices in the stiffness matrix $\mathbf{K}$ and mass matrix $\mathbf{M}$ are listed as follows.

$$
\begin{aligned}
\mathbf{H} &= [\cos\lambda_0 x \cos\lambda_0 y, \ldots, \cos\lambda_m x \cos\lambda_n y, \ldots, \\
&\quad \cos\lambda_M x \cos\lambda_N y, P_1(x)\cos\lambda_0 y, \ldots, P_l(x)\cos\lambda_n y, \\
&\quad \ldots, P_2(x)\cos\lambda_N y, P_1(y)\cos\lambda_0 x, \ldots, P_l(y)\cos\lambda_m x, \\
&\quad \ldots, P_2(y)\cos\lambda_M x] \\
\{\mathbf{K}_{uu}\} &= \int_0^a \int_0^b \left\{A_{11}\frac{\partial \mathbf{H}^{\mathbf{T}}}{\partial x}\frac{\partial \mathbf{H}}{\partial x} + A_{16}\frac{\partial \mathbf{H}^{\mathbf{T}}}{\partial x}\frac{\partial \mathbf{H}}{\partial y}\right. \\
&\quad \left. + A_{16}\frac{\partial \mathbf{H}^{\mathbf{T}}}{\partial y}\frac{\partial \mathbf{H}}{\partial x} + A_{66}\frac{\partial \mathbf{H}^{\mathbf{T}}}{\partial y}\frac{\partial \mathbf{H}}{\partial y}\right\} dy\,dx \\
&\quad + \int_0^b \left\{k_{x_0}^u \mathbf{H}^{\mathbf{T}}\mathbf{H}\big|_{x=0} + k_{x_1}^u \mathbf{H}^{\mathbf{T}}\mathbf{H}\big|_{x=a}\right\} dy \\
&\quad + \int_0^a \left\{k_{y_0}^u \mathbf{H}^{\mathbf{T}}\mathbf{H}\big|_{y=0} + k_{y_1}^u \mathbf{H}^{\mathbf{T}}\mathbf{H}\big|_{y=b}\right\} dx \\
\{\mathbf{K}_{vv}\} &= \int_0^a \int_0^b \left\{A_{22}\frac{\partial \mathbf{H}^{\mathbf{T}}}{\partial y}\frac{\partial \mathbf{H}}{\partial y} + A_{26}\frac{\partial \mathbf{H}^{\mathbf{T}}}{\partial x}\frac{\partial \mathbf{H}}{\partial y}\right. \\
&\quad \left. + A_{26}\frac{\partial \mathbf{H}^{\mathbf{T}}}{\partial y}\frac{\partial \mathbf{H}}{\partial x} + A_{66}\frac{\partial \mathbf{H}^{\mathbf{T}}}{\partial x}\frac{\partial \mathbf{H}}{\partial x}\right\} dy\,dx \\
&\quad + \int_0^b \left\{k_{x_0}^v \mathbf{H}^{\mathbf{T}}\mathbf{H}\big|_{x=0} + k_{x_1}^v \mathbf{H}^{\mathbf{T}}\mathbf{H}\big|_{x=a}\right\} dy \\
&\quad + \int_0^a \left\{k_{y_0}^v \mathbf{H}^{\mathbf{T}}\mathbf{H}\big|_{y=0} + k_{y_1}^v \mathbf{H}^{\mathbf{T}}\mathbf{H}\big|_{y=b}\right\} dx \\
\{\mathbf{K}_{ww}\} &= \int_0^a \int_0^b \left\{A_{44}\frac{\partial \mathbf{H}^{\mathbf{T}}}{\partial y}\frac{\partial \mathbf{H}}{\partial y} + A_{45}\frac{\partial \mathbf{H}^{\mathbf{T}}}{\partial x}\frac{\partial \mathbf{H}}{\partial y}\right. \\
&\quad \left. + A_{45}\frac{\partial \mathbf{H}^{\mathbf{T}}}{\partial y}\frac{\partial \mathbf{H}}{\partial x} + A_{55}\frac{\partial \mathbf{H}^{\mathbf{T}}}{\partial x}\frac{\partial \mathbf{H}}{\partial x}\right\} dy\,dx \\
&\quad + \int_0^b \left\{k_{x_0}^w \mathbf{H}^{\mathbf{T}}\mathbf{H}\big|_{x=0} + k_{x_1}^w \mathbf{H}^{\mathbf{T}}\mathbf{H}\big|_{x=a}\right\} dy \\
&\quad + \int_0^a \left\{k_{y_0}^w \mathbf{H}^{\mathbf{T}}\mathbf{H}\big|_{y=0} + k_{y_1}^w \mathbf{H}^{\mathbf{T}}\mathbf{H}\big|_{y=b}\right\} dx \\
\{\mathbf{K}_{\phi_x\phi_x}\} &= \int_0^a \int_0^b \left\{D_{11}\frac{\partial \mathbf{H}^{\mathbf{T}}}{\partial \phi_x}\frac{\partial \mathbf{H}}{\partial \phi_x} + D_{16}\frac{\partial \mathbf{H}^{\mathbf{T}}}{\partial \phi_x}\frac{\partial \mathbf{H}}{\partial y}\right. \\
&\quad + D_{16}\frac{\partial \mathbf{H}^{\mathbf{T}}}{\partial \phi_y}\frac{\partial \mathbf{H}}{\partial x} + D_{66}\frac{\partial \mathbf{H}^{\mathbf{T}}}{\partial y}\frac{\partial \mathbf{H}}{\partial y} + A_{55}\mathbf{H}^{\mathbf{T}}\mathbf{H}\left.\right\} dy\,dx \\
&\quad + \int_0^b \left\{k_{x_0}^x \mathbf{H}^{\mathbf{T}}\mathbf{H}\big|_{x=0} + k_{x_1}^x \mathbf{H}^{\mathbf{T}}\mathbf{H}\big|_{x=a}\right\} dy \\
&\quad + \int_0^a \left\{k_{y_0}^x \mathbf{H}^{\mathbf{T}}\mathbf{H}\big|_{y=0} + k_{y_1}^x \mathbf{H}^{\mathbf{T}}\mathbf{H}\big|_{y=b}\right\} dx \\
\left\{\mathbf{K}_{\phi_y\phi_y}\right\} &= \int_0^a \int_0^b \left\{D_{22}\frac{\partial \mathbf{H}^{\mathbf{T}}}{\partial \phi_y}\frac{\partial \mathbf{H}}{\partial \phi_y} + D_{26}\frac{\partial \mathbf{H}^{\mathbf{T}}}{\partial x}\frac{\partial \mathbf{H}}{\partial \phi_y}\right. \\
&\quad + D_{26}\frac{\partial \mathbf{H}^{\mathbf{T}}}{\partial \phi_y}\frac{\partial \mathbf{H}}{\partial x} + D_{66}\frac{\partial \mathbf{H}^{\mathbf{T}}}{\partial x}\frac{\partial \mathbf{H}}{\partial x} + A_{44}\mathbf{H}^{\mathbf{T}}\mathbf{H}\left.\right\} dy\,dx \\
&\quad + \int_0^b \left\{k_{x_0}^y \mathbf{H}^{\mathbf{T}}\mathbf{H}\big|_{x=0} + k_{x_1}^y \mathbf{H}^{\mathbf{T}}\mathbf{H}\big|_{x=a}\right\} dy \\
&\quad + \int_0^a \left\{k_{y_0}^y \mathbf{H}^{\mathbf{T}}\mathbf{H}\big|_{y=0} + k_{y_1}^y \mathbf{H}^{\mathbf{T}}\mathbf{H}\big|_{y=b}\right\} dx \\
\{\mathbf{K}_{uv}\} &= \int_0^a \int_0^b \left\{A_{12}\frac{\partial \mathbf{H}^{\mathbf{T}}}{\partial x}\frac{\partial \mathbf{H}}{\partial y} + A_{16}\frac{\partial \mathbf{H}^{\mathbf{T}}}{\partial x}\frac{\partial \mathbf{H}}{\partial x}\right. \\
&\quad \left. + A_{26}\frac{\partial \mathbf{H}^{\mathbf{T}}}{\partial y}\frac{\partial \mathbf{H}}{\partial y} + A_{66}\frac{\partial \mathbf{H}^{\mathbf{T}}}{\partial y}\frac{\partial \mathbf{H}}{\partial x}\right\} dy\,dx \\
\left\{\mathbf{K}_{u\phi_x}\right\} &= \int_0^a \int_0^b \left\{B_{11}\frac{\partial \mathbf{H}^{\mathbf{T}}}{\partial \phi_x}\frac{\partial \mathbf{H}}{\partial \phi_x} + B_{16}\frac{\partial \mathbf{H}^{\mathbf{T}}}{\partial \phi_x}\frac{\partial \mathbf{H}}{\partial y}\right. \\
&\quad \left. + B_{16}\frac{\partial \mathbf{H}^{\mathbf{T}}}{\partial y}\frac{\partial \mathbf{H}}{\partial \phi_x} + B_{66}\frac{\partial \mathbf{H}^{\mathbf{T}}}{\partial y}\frac{\partial \mathbf{H}}{\partial y}\right\} dy\,dx \\
\left\{\mathbf{K}_{u\phi_y}\right\} &= \int_0^a \int_0^b \left\{B_{12}\frac{\partial \mathbf{H}^{\mathbf{T}}}{\partial x}\frac{\partial \mathbf{H}}{\partial \phi_y} + B_{16}\frac{\partial \mathbf{H}^{\mathbf{T}}}{\partial x}\frac{\partial \mathbf{H}}{\partial x}\right. \\
&\quad \left. + B_{26}\frac{\partial \mathbf{H}^{\mathbf{T}}}{\partial \phi_y}\frac{\partial \mathbf{H}}{\partial \phi_y} + B_{66}\frac{\partial \mathbf{H}^{\mathbf{T}}}{\partial \phi_y}\frac{\partial \mathbf{H}}{\partial x}\right\} dy\,dx \\
\left\{\mathbf{K}_{v\phi_x}\right\} &= \int_0^a \int_0^b \left\{B_{12}\frac{\partial \mathbf{H}^{\mathbf{T}}}{\partial y}\frac{\partial \mathbf{H}}{\partial \phi_x} + B_{26}\frac{\partial \mathbf{H}^{\mathbf{T}}}{\partial y}\frac{\partial \mathbf{H}}{\partial y}\right. \\
&\quad \left. + B_{16}\frac{\partial \mathbf{H}^{\mathbf{T}}}{\partial \phi_x}\frac{\partial \mathbf{H}}{\partial \phi_x} + B_{66}\frac{\partial \mathbf{H}^{\mathbf{T}}}{\partial \phi_x}\frac{\partial \mathbf{H}}{\partial y}\right\} dy\,dx \\
\left\{\mathbf{K}_{v\phi_y}\right\} &= \int_0^a \int_0^b \left\{B_{22}\frac{\partial \mathbf{H}^{\mathbf{T}}}{\partial \phi_y}\frac{\partial \mathbf{H}}{\partial \phi_y} + B_{26}\frac{\partial \mathbf{H}^{\mathbf{T}}}{\partial \phi_y}\frac{\partial \mathbf{H}}{\partial x}\right. \\
&\quad \left. + B_{26}\frac{\partial \mathbf{H}^{\mathbf{T}}}{\partial x}\frac{\partial \mathbf{H}}{\partial \phi_y} + B_{66}\frac{\partial \mathbf{H}^{\mathbf{T}}}{\partial x}\frac{\partial \mathbf{H}}{\partial x}\right\} dy\,dx
\end{aligned}
$$

$$\left\{\mathbf{K}_{\phi_x\phi_y}\right\} = \int_0^a \int_0^b \left\{ D_{12}\frac{\partial \mathbf{H}^{\mathbf{T}}}{\partial \phi_x}\frac{\partial \mathbf{H}}{\partial \phi_y} + D_{16}\frac{\partial \mathbf{H}^{\mathbf{T}}}{\partial \phi_x}\frac{\partial \mathbf{H}}{\partial \phi_x} + D_{26}\frac{\partial \mathbf{H}^{\mathbf{T}}}{\partial \phi_y}\frac{\partial \mathbf{H}}{\partial \phi_y} + D_{66}\frac{\partial \mathbf{H}^{\mathbf{T}}}{\partial \phi_y}\frac{\partial \mathbf{H}}{\partial \phi_x} + A_{45}\mathbf{H}^{\mathbf{T}}\mathbf{H} \right\} dy\, dx$$

$$\left\{\mathbf{K}_{w\phi_x}\right\} = \int_0^a \int_0^b \left\{ A_{45}\frac{\partial \mathbf{H}^{\mathbf{T}}}{\partial \phi_y}\mathbf{H} + A_{55}\frac{\partial \mathbf{H}^{\mathbf{T}}}{\partial \phi_x}\mathbf{H} \right\} dy\, dx$$

$$\left\{\mathbf{K}_{w\phi_y}\right\} = \int_0^a \int_0^b \left\{ A_{44}\frac{\partial \mathbf{H}^{\mathbf{T}}}{\partial \phi_y}\mathbf{H} + A_{45}\frac{\partial \mathbf{H}^{\mathbf{T}}}{\partial \phi_x}\mathbf{H} \right\} dy\, dx$$

$$\left\{\mathbf{K}_{uw}\right\} = 0$$

$$\left\{\mathbf{K}_{vw}\right\} = 0$$

$$\mathbf{M}_{uu} = \mathbf{M}_{vv} = \mathbf{M}_{ww} = \int_0^a \int_0^b I_0 \mathbf{H}^{\mathrm{T}}\mathbf{H}\, dy\, dx$$

$$\mathbf{M}_{u\phi_x} = \mathbf{M}_{v\phi_y} = \int_0^a \int_0^b I_1 \mathbf{H}^{\mathrm{T}}\mathbf{H}\, dy\, dx$$

$$\mathbf{M}_{\phi_x\phi_x} = \mathbf{M}_{\phi_y\phi_y} = \int_0^a \int_0^b I_2 \mathbf{H}^{\mathrm{T}}\mathbf{H}\, dy\, dx \tag{B.1}$$

Data Availability

The data used to support the findings of this study are available from the corresponding author upon request.

Conflicts of Interest

The authors declare no conflicts of interest.

Acknowledgments

This project is supported by the Natural Science Foundation of Heilongjiang Province of China (Grant no. E2018019) and the Fundamental Research Funds for the Central Universities (Grant nos. HEUCFP201733 and HEUCFP201814).

References

[1] S. S. Vel and R. C. Batra, "Three-dimensional exact solution for the vibration of functionally graded rectangular plates," *Journal of Sound and Vibration*, vol. 272, no. 3–5, pp. 703–730, 2004.

[2] D. Liu, C. Wang, and W. Chen, "Free vibration of FGM plates with in-plane material inhomogeneity," *Composite Structures*, vol. 92, no. 5, pp. 1047–1051, 2010.

[3] I. A. Sidhoum, D. Boutchicha, S. Benyoucef, and A. Tounsi, "An original HSDT for free vibration analysis of functionally graded plates," *Steel and Composite Structures*, vol. 25, no. 6, pp. 735–745, 2017.

[4] S. Candiotti, J. L. Mantari, J. Yarasca, M. Petrolo, and E. Carrera, "An axiomatic/asymptotic evaluation of best theories for isotropic metallic and functionally graded plates employing non-polynomic functions," *Aerospace Science and Technology*, vol. 68, pp. 179–192, 2017.

[5] H. Li, F. Pang, X. Wang, and S. Li, "Benchmark solution for free vibration of moderately thick functionally graded sandwich sector plates on two-parameter elastic foundation with general boundary conditions," *Shock and Vibration*, vol. 2017, Article ID 4018629, 35 pages, 2017.

[6] Z. Su, G. Jin, and T. Ye, "Vibration analysis and transient response of a functionally graded piezoelectric curved beam with general boundary conditions," *Smart Materials and Structures*, vol. 25, no. 6, article no 14, Article ID 065003, 2016.

[7] Y. Q. Wang and J. W. Zu, "Porosity-dependent nonlinear forced vibration analysis of functionally graded piezoelectric smart material plates," *Smart Materials and Structures*, vol. 26, no. 10, 2017.

[8] L. Dai, T. Yang, J. Du, W. L. Li, and M. J. Brennan, "An exact series solution for the vibration analysis of cylindrical shells with arbitrary boundary conditions," *Applied Acoustics*, vol. 74, no. 3, pp. 440–449, 2013.

[9] D. N. Dinh and P. D. Nguyen, "The dynamic response and vibration of functionally graded carbon nanotube-reinforced composite (FG-CNTRC) truncated conical shells resting on elastic foundations," *Materials* , vol. 10, no. 10, 2017.

[10] S. Xiang, Z.-Y. Bi, S.-X. Jiang, Y.-X. Jin, and M.-S. Yang, "Thin plate spline radial basis function for the free vibration analysis of laminated composite shells," *Composite Structures*, vol. 93, no. 2, pp. 611–615, 2011.

[11] G. Jin, T. Ye, and S. Shi, "Three-dimensional vibration analysis of isotropic and orthotropic open shells and plates with arbitrary boundary conditions," *Shock and Vibration*, vol. 2015, Article ID 896204, 29 pages, 2015.

[12] Z. X. Lei, L. W. Zhang, and K. M. Liew, "Elastodynamic analysis of carbon nanotube-reinforced functionally graded plates," *International Journal of Mechanical Sciences*, vol. 99, pp. 208–217, 2015.

[13] H.-T. Xiao and Z.-Q. Yue, "Stresses and displacements in functionally graded materials of semi-infinite extent induced by rectangular loadings," *Materials* , vol. 5, no. 2, pp. 210–226, 2012.

[14] S.-H. Chi and Y.-L. Chung, "Mechanical behavior of functionally graded material plates under transverse load - Part II: numerical results," *International Journal of Solids and Structures*, vol. 43, no. 13, pp. 3675–3691, 2006.

[15] S. Chi and Y. Chung, "Mechanical behavior of functionally graded material plates under transverse load—part I: analysis," *International Journal of Solids and Structures*, vol. 43, no. 13, pp. 3657–3674, 2006.

[16] S. Akhlaque-E-Rasul and R. Ganesan, "The compressive response of thickness-tapered shallow curved composite plates based on classical shell theory," *Journal of Advanced Materials*, vol. 43, no. 1, pp. 47–65, 2011.

[17] T. Ye, G. Jin, S. Shi, and X. Ma, "Three-dimensional free vibration analysis of thick cylindrical shells with general end conditions and resting on elastic foundations," *International Journal of Mechanical Sciences*, vol. 84, pp. 120–137, 2014.

[18] L. F. Qian, R. C. Batra, and L. M. Chen, "Static and dynamic deformations of thick functionally graded elastic plates by using higher order shear and normal deformable plate theory and meshless local Petrov-Galerkin method," *Composites Part B: Engineering*, vol. 35, no. 6–8, pp. 685–697, 2004.

[19] F. Tornabene, S. Brischetto, N. Fantuzzi, and E. Viola, "Numerical and exact models for free vibration analysis of cylindrical

and spherical shell panels," *Composites Part B: Engineering*, vol. 81, pp. 231–250, 2015.

[20] T. Naskar and J. Kumar, "Predominant modes for Rayleigh wave propagation using the dynamic stiffness matrix approach," *Journal of Geophysics and Engineering*, vol. 14, no. 5, pp. 1032–1041, 2017.

[21] Y. Chen, G. Chen, and X. Xie, "Weak Galerkin finite element method for Biot's consolidation problem," *Journal of Computational and Applied Mathematics*, vol. 330, pp. 398–416, 2018.

[22] J. Rouzegar and A. Abbasi, "A refined finite element method for bending of smart functionally graded plates," *Thin-Walled Structures*, vol. 120, pp. 386–396, 2017.

[23] F. Tornabene, N. Fantuzzi, and M. Bacciocchi, "The GDQ method for the free vibration analysis of arbitrarily shaped laminated composite shells using a NURBS-based isogeometric approach," *Composite Structures*, vol. 154, pp. 190–218, 2016.

[24] Y. Kiani, R. Dimitri, and F. Tornabene, "Free vibration of FG-CNT reinforced composite skew cylindrical shells using the Chebyshev-Ritz formulation," *Composites Part B: Engineering*, vol. 147, pp. 169–177, 2018.

[25] F. Tornabene, N. Fantuzzi, and M. Bacciocchi, "A new doubly-curved shell element for the free vibrations of arbitrarily shaped laminated structures based on weak formulation isogeometric analysis," *Composite Structures*, vol. 171, pp. 429–461, 2017.

[26] R. Vaghefi, G. H. Baradaran, and H. Koohkan, "Three-dimensional static analysis of thick functionally graded plates by using meshless local Petrov-Galerkin (MLPG) method," *Engineering Analysis with Boundary Elements*, vol. 34, no. 6, pp. 564–573, 2010.

[27] H. Wu, S. Kitipornchai, and J. Yang, "Thermo-electro-mechanical postbuckling of piezoelectric FG-CNTRC beams with geometric imperfections," *Smart Materials and Structures*, vol. 25, no. 9, 2016.

[28] M. Aghelinejad, K. Zare, F. Ebrahimi, and A. Rastgoo, "Nonlinear thermomechanical post-buckling analysis of thin functionally graded annular plates based on Von-Karman's plate theory," *Mechanics of Advanced Materials and Structures*, vol. 18, no. 5, pp. 319–326, 2011.

[29] M. M. Alipour and M. Shariyat, "Analytical stress analysis of annular FGM sandwich plates with non-uniform shear and normal tractions, employing a zigzag-elasticity plate theory," *Aerospace Science and Technology*, vol. 32, no. 1, pp. 235–259, 2014.

[30] A. Allahverdizadeh, M. H. Naei, and M. Nikkhah Bahrami, "Vibration amplitude and thermal effects on the nonlinear behavior of thin circular functionally graded plates," *International Journal of Mechanical Sciences*, vol. 50, no. 3, pp. 445–454, 2008.

[31] Y. Chen, G. Jin, and Z. Liu, "Free vibration analysis of circular cylindrical shell with non-uniform elastic boundary constraints," *International Journal of Mechanical Sciences*, vol. 74, pp. 120–132, 2013.

[32] W. L. Li, X. Zhang, J. Du, and Z. Liu, "An exact series solution for the transverse vibration of rectangular plates with general elastic boundary supports," *Journal of Sound & Vibration*, vol. 321, no. 1-2, pp. 254–269, 2009.

[33] D. P. Zhang, Y. J. Lei, and Z. B. Shen, "Thermo-electro-mechanical vibration analysis of piezoelectric nanoplates resting on viscoelastic foundation with various boundary conditions," *International Journal of Mechanical Sciences*, vol. 131-132, pp. 1001–1015, 2017.

[34] M. O. Yayli, "An efficient solution method for the longitudinal vibration of nanorods with arbitrary boundary conditions via a hardening nonlocal approach," *Journal of Vibration and Control*, vol. 24, no. 11, pp. 2230–2246, 2018.

[35] M. Sekkal, B. Fahsi, A. Tounsi, and S. R. Mahmoud, "A novel and simple higher order shear deformation theory for stability and vibration of functionally graded sandwich plate," *Steel and Composite Structures*, vol. 25, no. 4, pp. 389–401, 2017.

[36] V. Alankaya and A. S. Oktem, "Static analysis of laminated and sandwich composite doubly-curved shallow shells," *Steel and Composite Structures*, vol. 20, no. 5, pp. 1043–1066, 2016.

[37] M. Yaqoob Yasin and S. Kapuria, "An efficient layerwise finite element for shallow composite and sandwich shells," *Composite Structures*, vol. 98, pp. 202–214, 2013.

[38] R. Talebitooti, K. Daneshjou, and A. Tarkashvand, "Study of imperfect bonding effects on sound transmission loss through functionally graded laminated sandwich cylindrical shells," *International Journal of Mechanical Sciences*, vol. 133, pp. 469–483, 2017.

[39] Y. Hao, Z. Li, W. Zhang, S. Li, and M. Yao, "Vibration of functionally graded sandwich doubly curved shells using improved shear deformation theory," *Science China Technological Sciences*, vol. 61, no. 6, pp. 791–808, 2018.

[40] A. H. Sofiyev, "Application of the FOSDT to the solution of buckling problem of FGM sandwich conical shells under hydrostatic pressure," *Composites Part B: Engineering*, vol. 144, pp. 88–98, 2018.

[41] M.-C. Trinh and S.-E. Kim, "Nonlinear thermomechanical behaviors of thin functionally graded sandwich shells with double curvature," *Composite Structures*, vol. 195, pp. 335–348, 2018.

[42] Q. Li, V. P. Iu, and K. P. Kou, "Three-dimensional vibration analysis of functionally graded material sandwich plates," *Journal of Sound and Vibration*, vol. 311, no. 1-2, pp. 498–515, 2008.

[43] L. Hadji, H. A. Atmane, A. Tounsi, I. Mechab, and E. A. Adda Bedia, "Free vibration of functionally graded sandwich plates using four-variable refined plate theory," *Applied Mathematics and Mechanics-English Edition*, vol. 32, no. 7, pp. 925–942, 2011.

[44] G. Jin, S. Shi, Z. Su, S. Li, and Z. Liu, "A modified Fourier–Ritz approach for free vibration analysis of laminated functionally graded shallow shells with general boundary conditions," *International Journal of Mechanical Sciences*, vol. 93, pp. 256–269, 2015.

[45] T. Ye, G. Jin, Y. Chen, X. Ma, and Z. Su, "Free vibration analysis of laminated composite shallow shells with general elastic boundaries," *Composite Structures*, vol. 106, pp. 470–490, 2013.

[46] T. Erber, "Hooke's law and fatigue limits in micromechanics," *European Journal of Physics*, vol. 22, no. 5, pp. 491–499, 2001.

[47] D. Gallistl, P. Huber, and D. Peterseim, "On the stability of the Rayleigh–Ritz method for eigenvalues," *Numerische Mathematik*, vol. 137, no. 2, pp. 339–351, 2017.

[48] Y. Fu, J. Yao, Z. Wan, and G. Zhao, "Free vibration analysis of moderately thick orthotropic functionally graded plates with general boundary restraints," *Materials* , vol. 11, no. 2, 2018.